

**EFFECTS OF BORONIZING ON SHARP CORNERED
METAL SURFACE**

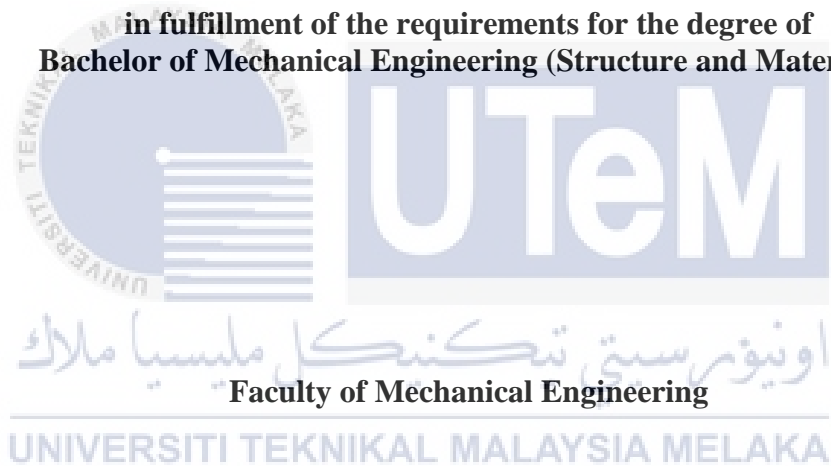


UNIVERSITI TEKNIKAL MALAYSIA MELAKA

**EFFECTS OF BORONIZING ON SHARP CORNERED
METAL SURFACE**

NABILAH BINTI AB HALIM

**This thesis is submitted
in fulfillment of the requirements for the degree of
Bachelor of Mechanical Engineering (Structure and Materials)**




UNIVERSITI TEKNIKAL MALAYSIA MELAKA

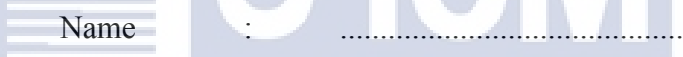
JUNE2017

DECLARATION


I declare that this project report entitled “Effects of Boronizing on Sharp Cornered Metal Surface” is the result of my own work except as cited in the references





Signature :



Name :



Date :



UNIVERSITI TEKNIKAL MALAYSIA MELAKA

APPROVAL

I hereby declare that I have read this project report and in my opinion this report is sufficient in terms of scope and quality for the award of the degree of Bachelor of Mechanical Engineering (Structure & Materials).



Signature :

Name of Supervisor :
اونيورسيتي تيكنيكل ماليزيا ملاك

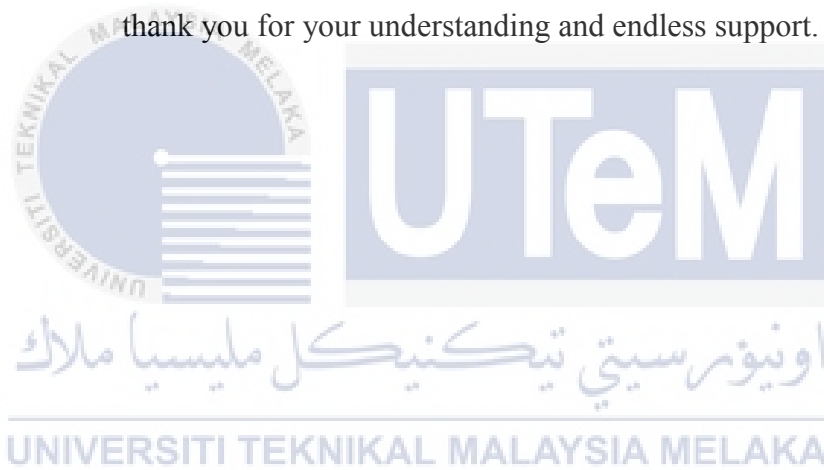
Date :

UNIVERSITI TEKNIKAL MALAYSIA MELAKA

DEDICATION

To my beloved mother, bah and family,

thank you for your understanding and endless support.



ABSTRACT

Boronizing is a thermochemical process usually used to harden the material. Based on published previous researches, boronizing process was studied but only focusing on the hardening of the material. This study is focusing on the boronizing process on the cornered of the metal surface. In this study, the sharp cornered surface will be studied in order to know which part of the geometries that shows the most effective boronizing process by using two parameters that are temperature and time. The parameters are 850°C - 950°C (1123K – 1223K) for 2, 4 and 6 hours. Besides that, this study is to analyse the effect of different cornered geometries by using the activation energy. There are four different geometries at each corner of the metal specimen that are 90°, 1mm fillet, 5mm radius, and chamfer. The specimens need to be designed and fabricated with the dimension of 20mm X 20mm X 20 mm to suit into the existing container. After the boronizing process has been done, metallographic analyses were used to determine the boride layer thickness. From the boride layer thickness, the activation can be calculated and the geometry with lowest activation energy is the best shape and the boron is easy to diffuse. As the conclusion, the 90° geometry has the lowest activation energy with value of 61.785 kJ/mol.

ABSTRAK

Boronizing adalah satu proses termokimia biasanya digunakan untuk mengeraskan bahan. Berdasarkan kajian sebelum diterbitkan, proses boronizing dikaji tetapi hanya memberi tumpuan kepada pengerasan bahan. Dalam kajian ini, proses penyusukboronan di penjuru permukaan logam akan diberi tumpuan. Dalam kajian ini, permukaan penjuru yang tajam akan dikaji untuk mengetahui bentuk geometri yang menunjukkan proses penyusukboronan yang paling berkesan dengan menggunakan dua parameter iaitu suhu dan masa. Parameternya adalah 850°C - 950°C (1123K - 1223K) selama 2, 4 dan 6 jam. Selain itu, kajian ini adalah untuk menganalisis kesan geometri pada penjuru yang berbeza dengan menggunakan tenaga pengaktifan. Terdapat empat geometri yang berbeza pada setiap sudut spesimen logam iaitu 90° , fillet 1mm, jejari 5mm, dan talang. Spesimen perlu direka terlebih dahulu dengan dimensi 20mm X 20mm X 20 mm untuk disesuaikan ke dalam bekas yang sedia ada. Selepas proses penyusukboronan itu telah dilakukan, analisis metallographic digunakan untuk menentukan ketebalan lapisan boron. Daripada ketebalan lapisan boron yang diperolehi, tenaga pengaktifan boleh dikira dan geometri yang mempunyai tenaga pengaktifan paling rendah adalah bentuk yang terbaik dan boron mudah untuk meresap. Sebagai kesimpulan, geometri 90° mempunyai tenaga pengaktifan yang paling rendah dengan nilai 61,785 kJ / mol.

ACKNOWLEDGEMENTS

First of all thanks to Almighty Allah for giving me strength and ability to complete this study report.

I would like to express my deepest appreciation to my supervisor, Dr. Rafidah Hasan for giving me this opportunity to do final year project with her and her endless advice, suggestion and guidance whenever for this whole study. I am thankful for his patience and advice while leading me in this study.

Next, I would like to thank this appreciation laboratory staff En. Mazlan and En. Mahader for his kindness in giving suggestions to me and spare their time to help me in conducting the laboratory equipment.

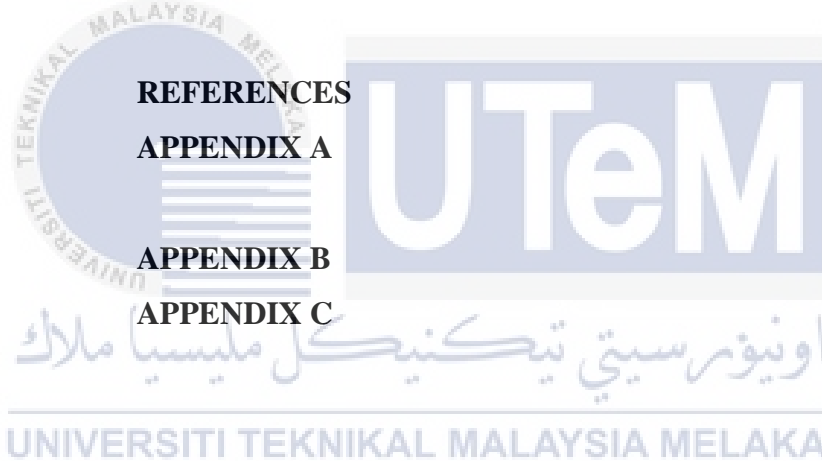
I would like to thank my family for their moral support when I needed. Finally, I would like to thank my course mates for giving me their support and encouragement throughout this study.

CONTENT

CHAPTER	CONTENT	PAGE
	DECLARATION	ii
	APPROVAL	iii
	DEDICATION	iv
	ABSTRACT	v
	ABSTRAK	vi
	ACKNOWLEDGEMENTS	vii
	TABLE OF CONTENT	viii
	LIST OF ABBREVIATION	xi
	LIST OF FIGURE	xii
	LIST OF TABLE	xv
	LIST OF SYMBOL	xvii
	LIST OF APPENDICES	xviii
CHAPTER 1	INTRODUCTION	1
	1.1 Background	1
	1.2 Problem Statement	2
	1.3 Objective	3
	1.4 Scope of Project	3
CHAPTER 2	LITERATURE REVIEW	4
	2.1 Background of Steel	4
	2.1.1 Types of Steel	5
	2.2 Background of Mild Steel	7
	2.3 Background of Boronizing	8

2.3.1	Types of Boronizing	10
2.3.2	Application of Boronizing	11
2.3.3	Advantages and Disadvantages of Boronizing	11
2.4	Microscopy	12
2.4.1	Optical Microscopy	12
2.4.2	Scanning Electron Microscopy (SEM)	13
2.5	Activation Energy	14
2.5.1	Arrhenius Equation	16
CHAPTER 3	METHODOLOGY	17
3.1	Introduction	17
3.2	Project Flow Chart	18
3.3	Material	19
3.4	Specimens	19
3.4.1	Design of specimen	19
3.4.2	Fabrication	20
3.5	Boronizing Process	24
3.5.1	Preparation	24
3.5.2	Process	25
3.6	Material Characterization	27
3.7	Activation Energy	30
3.7.1	Arrhenius Equation	30
3.8	Preliminary Result	32
CHAPTER 4	DATA AND RESULT	34
4.1	Introduction	34
4.2	Microstructure	35
4.2.1	Data	40
4.2.2	Graph	42
4.3	Kinetic Of Boron Diffusion	45
4.3.1	90° Geometry	45
4.3.2	1mm Fillet	47
4.3.3	5mm Radius	49

4.3.4	Chamfer	51
4.4	Activation Energy	532
CHAPTER 5	DISCUSSION AND ANALYSIS	54
5.1	Introduction	54
5.2	Microstructure Analysis	55
5.3	Boride Layer Thickness Analysis	56
5.4	Kinetic Of Atom Diffusion Analysis	56
CHAPTER 6	CONCLUSION AND RECOMMENDATIONS	59
6.1	Introduction	59
6.2	Conclusion	60
6.3	Recommendations	61
	REFERENCES	61
	APPENDIX A	A1
	APPENDIX B	B
	APPENDIX C	C1
		C2



LIST OF ABBEREVATIONS

ANSI	American Iron and Steel Institution
ASTM	American Society for Testing and Materials
AISI	American Iron and Steel Institute
SEM	Scanning Electron Microscopy
2H	2 Hours
4H	4 Hours
6H	6 Hours



اونيورسيتي تيكنيكل مليسيا ملاك

UNIVERSITI TEKNIKAL MALAYSIA MELAKA

LIST OF FIGURES

FIGURE	TITLE	PAGE
2.1	Optical Microscopy	13
2.2	Diagram of SEM column and specimen chamber	14
3.1	Flow chart of the methodology	18
3.2	Mild steel	19
3.3(a)	Design of sharp cornered surface specimen	20
3.3(b)	Top view of the design	20
3.4(a)	Bandsaw machine	21
3.4(b)	Cutting materials using bandsaw machine	21
3.5	Steel block	21
3.6	Material to be cut using handsaw	22
3.7	CNC milling machine	22
3.8	Specimen before and after CNC milling machine process	23
3.9	Finishing surface after grinding	23
3.10(a)	Fill up the boronizing powder in container	23
3.10(b)	Specimens in container with boronizing powders	24
3.10(c)	Schematic diagrams for boronizing preparation	25

3.11(a)	Furnace	25
3.11(b)	Furnace	26
3.12	Hot container removed from furnace	26
3.13	Schematic diagram of boronizing process	26
3.14	Grinding specimen	27
3.15	Optical microscope	28
3.16	Basic steps for specimen preparation-microscopy.	29
3.17	Boride layer against the boronizing time	31
3.18	Boride layer morphology	31
3.19	SEM micrographs of borided steel	33
4.1 (a)	Micrographs of the geometries for 2H at 850 °C	35
4.1 (b)	Micrographs of the geometries for 4H at 850 °C	35
4.1 (c)	Micrographs of the geometries for 6H at 850 °C	36
4.2 (a)	Micrographs of the geometries for 2H at 900 °C	36
4.2 (b)	Micrographs of the geometries for 4H at 900 °C	37
4.2 (c)	Micrographs of the geometries for 6H at 900 °C	37
4.3 (a)	Micrographs of the geometries for 2H at 950 °C	38
4.3 (b)	Micrographs of the geometries for 4H at 950 °C	38
4.3 (c)	Micrographs of the geometries for 6H at 950 °C	39
4.4 (a)	Graph of boride layers against boronizing time for 90°	43
4.4 (b)	Graph of boride layers against boronizing time for 1mm fillet	43
4.4 (c)	Graph of boride layers against boronizing time for 5mm radius	44

4.4 (d)	Graph of boride layers against boronizing time for chamfer	44
4.5 (a)	Squared boride layer against boronizing time for 90°	45
4.5 (b)	Squared boride layers against boronizing time for fillet	47
4.5 (c)	Squared boride layers against boronizing time for 5mm radius	49
4.5 (d)	Squared boride layer against boronizing time for chamfer	51
4.6 (a)	Natural logarithm of growth rate constant ($\ln k$) as a function of reciprocal boronizing temperature ($1/T$) for 90°	46
4.6 (b)	Natural logarithm of growth rate constant ($\ln k$) as a function of reciprocal boronizing temperature ($1/T$) for 1mm fillet	48
4.6 (c)	Natural logarithm of growth rate constant ($\ln k$) as a function of reciprocal boronizing temperature ($1/T$) for 5mm radius	50
4.6 (d)	Natural logarithm of growth rate constant ($\ln k$) as a function of reciprocal boronizing temperature ($1/T$) for chamfer	52
5.1	SEM micrographs of borided steel at 950 C for (c) 2 h, (d) 8 h	55
5.2	Micrographs of the geometries for 2H at 950 °C	55
5.3	Chart for gradient of geometries	57
5.4	Graph of activation energy for four geometries	58

LIST OF TABLE

TABLE	TITLE	PAGE
2.1	Carbon contain for three groups of Carbon Steel	5
2.2	Types of Stainless Steels with the properties	6
2.3	Steel products divided by the shapes and related applications	7
2.4	Composition, properties and uses of ferrous metals	8
2.5	Properties of Boride	9
2.6	Application of boronizing in industry	11
2.7	Advantages and disadvantages of boronizing process	12
2.8	Typical characteristics of diffusion treatments	15
4.1(a)	Thickness for 90° at cornered geometry	40
4.1(b)	Thickness for 1mm fillet cornered geometry	41
4.1(c)	Thickness for 5mm radius at cornered geometry	41
4.1(d)	Thickness for chamfer cornered geometry	42
4.2 (a)	Thickness data for 90°	45
4.2 (b)	Thickness data for 1mm fillet	47
4.2 (c)	Thickness data for 5mm radius	49
4.2 (d)	Thickness data for chamfer	51

4.3 (a)	Gradient of each temperature for 90°	46
4.3 (b)	Gradient of each temperature for 1mm fillet	48
4.3 (c)	Gradient of each temperature for 5mm radius	50
4.3 (d)	Gradient of each temperatures for chamfer	52
4.4 (a)	Data of ln k and 1/T for 90°	46
4.4 (b)	Data of ln K and 1/T for 1mm fillet	48
4.4 (c)	Data of ln K and 1/T for 5mm radius	50
4.4 (d)	Data of ln K and 1/T for chamfer	52
4.5	Result for the activation energy for geometries	53



LIST OF SYMBOL

k	Rate constant
E_a	Activation energy
R	Gas constant
T	Temperature in Kelvin
A	Arrhenius constant
d	The depth of boride layer



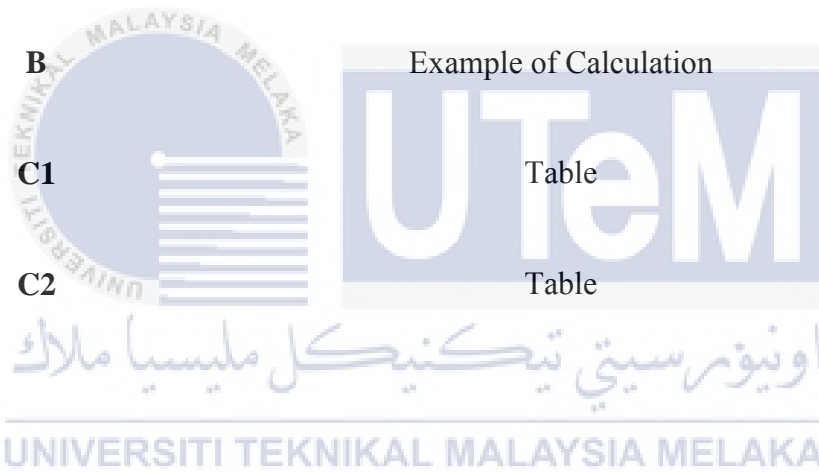
اونيورسيتي تيكنيكل مليسيا ملاك

UNIVERSITI TEKNIKAL MALAYSIA MELAKA

LIST OF APPENDICES

APPENDIX	TITLE
A1	Gantt Charts For Psm 1
A2	Gantt Charts For Psm 2

B	Example of Calculation
C1	Table
C2	Table



UNIVERSITI TEKNIKAL MALAYSIA MELAKA

CHAPTER 1

INTRODUCTION

1.1 Background

Boronizing is a broadly utilized thermochemical preparing system for surface adjustment. The surface adjustment such as surface hardening is where the boron is diffused into the material's surface at high temperature. This procedure has connected to an extensive variety of materials, for example, ferrous or non-ferrous composites, and cermet and the end goal is to enhance their solidness and mechanical execution (He et al., 2015). Boronizing can be produced by using blends of powders, salts, liquid oxides, and additionally gas mediums and glues (Campos et al., 2007). The temperature of this process is usually within the range of 700°C to 1000°C for 1 to 12 hours. The capacity of boronizing is to boost the wear execution, hardness and erosion for the material and segment in modern applications.

The attributes of this boride layer rely on upon the physical condition of the boron source utilized, the boronizing temperature, the treatment time, and the concoction piece of the material to be borided (Chegroune et al., 2016). It is realized that boronizing performed at high temperature is a dissemination controlled process. It is vital to set up the procedure parameters that influence the boronizing energy with a specific end goal to choose prepare parameters to accomplish the sought thickness of boride layer and hardness (Genel et al., 2003).

Boride has a high melting point and high hardness at elevated temperatures and, consequently is the basic advantage of boriding. Based on the researches of the boriding in transition metals, it have accelerated particularly for the applications in the production of cutting tools and heavy gears, and in the automotive, casting, textile, food-processing, packaging and ceramic industries where huge friction-dependent energy losses and intensive corrosion and wear occur (Gunes, et al., 2015).

A high temperature is essential for boronization because of two facts: 1) heat-induced formation of vacancies in the matrix and 2) activation of boron atoms to overcome the energy barrier for diffusion. Conventional boronizing processes for ferrous were conducted at temperatures around ~ 1000 °C (He et al., 2015).

This study, will focus on the effect of boronizing on the sharp cornered surface. There will be four geometries for each sharp cornered surface and the boronizing process will be held using two parameters. The parameter uses are temperature and time. The ranges of the temperature that will be used are 850°C, 900°C and 950°C while the time is 2, 4 and 6 hours. The result after boronizing process will be used to evaluate the diffusion by the boride layer thickness and activation energy analysis.

UNIVERSITI TEKNIKAL MALAYSIA MELAKA

1.2 Problem Statement

In engineering there are many things that are important such as designs, build, improve structures, machines, tools, components and materials. Boronizing is one of the processes that available in engineering field. Based on published previous researches, boronizing process was studied but only focusing on the hardening of the material. In this study, the sharp cornered surface will be studied in order to know which part of the geometries that shows the most effective boronizing process by analyzing the rate of diffusion.

1.3 Objectives

The objectives of this study are as follows:

1. To study the effect of boronizing in temperature and time on the sharp cornered surface using the metallographic analysis.
2. To analyse the effect of different cornered geometries on the boronizing diffusion using the activation energy analysis.

1.4 Scope of Project

The scope of this study including:

1. Design and fabricate a suitable dimension for the specimen to suit the container that available
2. Determine the thickness of the boride layer by using the metallographic analysis.
3. The activation energy will be analysed by using Arrhenius Eq.

CHAPTER 2

LITERATURE REVIEW

2.1 Background of Steel

Based on the World Steel Association, it have been recorded that the steel grades are more than 3,500 types, environmental properties, encircling unique physical and chemical (About steel, 2016). In quintessence, the steel is composed of iron and carbon. The properties of each steel grade can be determined by the amount of carbon and additional alloying element as well as the level of impurities. The amount of carbon contents in steel are in the range of 0.1-0.25% carbon. However, the carbon content of 0.1-0.25% usually used in steel that is widely used in the industry. In all grades of steel, there are any other elements such as manganese, phosphorus and also sulphur. The manganese offers beneficial effects while the phosphorous and sulfur is harmful for the strength and durability of steel (Bell, 2016).

There are different types of standard in the industries and one of it is the standard for steel. American Iron and Steel Institution (ANSI), American Society for Testing and Materials (ASTM) for steel standard are used for different types of steels to categorizing, properties of metallurgical, evaluation, specifying of material, chemical, and mechanical. The steel standard is useful for guiding in metallurgical laboratories and refineries, manufacturing the product, and for end-users of steel. In order to ensure the quality towards the safe of use, the modifications for the steel must be in proper process and application procedure (ASTM, 1998-2016).

Steel have been widely used in production industries such as automobile, shipbuilding, the construction, canned foods, electrical appliances, surgical instruments and many more (Bell, 2016).

2.1.1 Types of Steel

There are different types of steel produce based on the properties that are required for the application and several grading systems that are used to differentiate the steel based on the properties. Based on the American Iron and Steel Institute (AISI), there are four group of chemical composition that used to categorize the steel (Bell, 2016). The groups are as follows:

- 
- i) Carbon Steels
 - ii) Alloys Steels
 - iii) Stainless Steels
 - iv) Tools Steels

i) Carbon Steels
 For Carbon steels, its contain traces amounts of alloying elements. According to the carbon content, the carbon steel can be further categorized into three groups as in Table 2.1.

Table 2.1: Carbon contain for three groups of Carbon Steel
 (Source: Bell, 2016)

Types of Steel	Carbon Contain
Low Carbon Steels/Mild Steels	up to 0.3%
Medium Carbon Steels	0.3 – 0.6%
High Carbon Steels	more than 0.6%

ii) Alloys Steels

Alloy steel contains alloying element such as nickel, copper, chromium and aluminium in varying proportions to manipulate the properties of the steel. The properties of steel are such as corrosion resistance, strength, formability, hardenability, weldability or ductility. Alloy steel can be used in pipelines, auto parts, power generators and electric motors (Bell, 2016).

iii) Stainless Steels

For Stainless steels it basically contains chromium as the main alloying element between 10-20% and it is valued for high corrosion resistance. Steel is more resistant about 200 times to corrosion than mild steel with over 11% chromium (Bell, 2016). These steels can be divided into three groups based on their crystalline structure as in Table 2.2.

Table 2.2 Types of Stainless Steels with the properties
(Source: Bell, 2016)

Types of Stainless Steels	Properties
Austenitic	<ul style="list-style-type: none"> • 18% chromium • 8% nickel • Less than 0.8% carbon
Ferritic	<ul style="list-style-type: none"> • Contain trace amounts of nickel • 12-17% chromium • Less than 0.1% carbon • Other alloying elements, such as molybdenum, aluminum or titanium
Martensitic	<ul style="list-style-type: none"> • 11-17% chromium • Less than 0.4% nickel • 1.2% carbon

iv) Tools Steels

Tungsten, molybdenum, cobalt and vanadium in varying quantities are the tool steels contain. The functions are to increase heat resistance and durability, make it suitable for cutting and drilling equipment. Steel products can be divided by the shapes and related applications as in Table 2.3 (Bell, 2016).

Table 2.3 Steel products divided by the shapes and related applications
(Source: Bell, 2016)

Product	Shape	Application
Long/Tubular	<ul style="list-style-type: none"> • Bars and rods • Rails • Wires • Angles • Pipes • Shapes 	<ul style="list-style-type: none"> • Automotive • Construction sectors
Flat	<ul style="list-style-type: none"> • Plates • Sheets • Coils • Strips 	<ul style="list-style-type: none"> • Automotive parts • Appliances • Packaging • Shipbuilding • Construction.
Other	<ul style="list-style-type: none"> • Valves • Fittings • Flanges 	<ul style="list-style-type: none"> • Piping materials

2.2 Background of Mild Steel

Metal is consists of ferrous metal and non-ferrous metal. Mild steel is one of the ferrous metals. Ferrous metal containing iron and the carbon contain are up to 0.3% (Metal, 2012). Table 2.4 below shows the composition, properties and uses of ferrous metals.

Table 2.4: Composition, properties and uses of ferrous metals.

(Source: Educastur, 2009)

Name	Composition	Properties and characteristics	Principal uses
Cast iron	Alloy of iron and 2-5% carbon, 1-3% silicon and traces of magnesium, sulphur and phosphorus.	Hard skin, softer underneath, but brittle. It corrodes by rusting.	Parts with complex shapes which can be made by casting
Mild steel	Alloy of iron and 0.15 - 0.3% carbon	Tough, ductile and malleable. Good tensile strength, poor resistance to corrosion	General-purpose engineering material
Medium carbon steel	Alloy of iron and 0.35 - 0.7% carbon	Strong, hard and tough, with a high tensile strength, but less ductile than mild steel.	Springs; any application where resistance to wear is needed
High carbon steel	Alloy of iron and carbon: 0.7 - 1.5% carbon	Even harder than medium carbon steel, and more brittle. Can be heat-treated to make it harder and tougher	Cutting tools, mechanical elements
Stainless steel	Alloy of iron and carbon with 16-26% chromium, 8-22% nickel and 8% magnesium	Hard and tough, resists wear and corrosion	Cutlery, kitchen equipment
High speed steel	Alloy of iron and 0.35 - 0.7% carbon (medium carbon steel) with tungsten, chromium, vanadium, and sometimes cobalt	Very hard, high abrasion- and heat-resistance	Cutting tools for machines

2.3 Background of Boronizing

Wide range of application is one of the main reasons of boronizing process widely used in the industry. 700 °C to 1000 °C for 1-12 hours is the range for thermochemical treatment commonly achieved. The boronizing process brings about a metallic boride layer of about 20 µm – 300 µm thicknesses. For ferrous materials, the boronizing treatment leads to the growth of either a single layer (Fe₂B) or double-layer (FeB+Fe₂B) with a certain composition. The characteristics of boride layer depend on the physical state of the boron source used, the temperature of boronizing, the time of treatment, and the chemical composition of the boride material. The thickness of the boride layer will be increase as the temperature increased (Chegroune et al, 2016).

Boronizing is an effective method for significantly mounting the surface hardness and the wear resistance of metals. Generally a boron compound layer is developed on the surface of boronized ferrous alloys. The boride layer commonly composed in two sublayers that are the outermost and innermost which contained FeB and Fe₂B respectively. This is because of the diffusion zone hardly exists due to the very small solubility of boron in Fe. Meanwhile, the FeB phase is more brittle and harder, and it has higher coefficient of thermal expansion than the Fe₂B one. Then, the cracking of the double-phase boride layer is often observed (Béjar & Moreno, 2006).

Boronizing can be performed at high temperature and it is a diffusion-controlled process. It is very important to establish the process parameters that affect the boriding kinetics in order to select process parameters to attain the desired thickness of boride layer and hardness. (Genel et al, 2003). Carburizing, nitriding or carbonitriding are superior alternative process for conventional surface hardening processes that can be offered by the boronizing (Yu et al, 2002). The properties of the boronizing are as in Table 2.5.

Table 2.5: Properties of Boride

(Source: Avion, 2016)

	FeB	Fe₂B
% Bor	16,23	8,83
Lattice Structure	rhombic	tetragonal
Stress after cooling down	Tension	Compressive
Coefficient of Linear Expansion 10 ⁻⁶ /K	23	7,9-9,2
Hardness [HV0.1]	1900-2100	1650-2000
Density [g/cm ³]	6,75	7,43
Modulus of Elasticity [GPa]	343	284
Thermal Conductivity [W/mK]	12	30

2.3.1 Types of Boronizing

The boronizing treatment can be carried out either in solid, liquid, gas or plasma state (Chegroune et al, 2016).

i. Solid

The pack boronizing known as the solid treatment is the low cost process in engineering industry. This is because it is an easy process and not complicated. Pack boronizing process use powder or paste for boronizing. The material or specimen that will be borided will be immersed in the container with the boron powder, and it is heated until determined temperature and time. (Davis, 2002).

An alternative method of powder boronizing process is the paste boronizing process. Paste boronizing is useful in high volume work. This is because the paste is more convenient in the discerning boronizing process. The boron paste can only be used in a controlled atmosphere where it determines the thickness of the boride layer (Campos et al., 2003).

ii. Gas

Gas boronizing is one of the thermochemical treatments such as carburizing and nitriding process and it is more economically effective. However, because of toxicity or corrosion these processes are not used commercially (Küper et al, 2000).

iii. Plasma


In plasma boriding, material or specimen that will be boriding will be placed in a vacuum chamber. After the material or specimen have been inserted in the chamber, the chamber is pre-heated with a mixture of inert gas by an electrical power (Yang et al, 2013).

2.3.2 Application of Boronizing

Boronizing is the process that is widely used (Campos et al., 2003). The Table 2.6 below shows the application of boronizing for the industries.

Table 2.6: Applications of boronizing in industry.

(Source: Avion, 2016)

 <p>Application of Boronizing</p>	Automotive component
	Oil and gas industry <ul style="list-style-type: none"> • Valve • Accessories
	Power plant engineering
	Tool making and metal forming technology
	Plastics processing
	Glass production
	Gear manufacturing
	Component for textile machinery
	Mechanical engineering

2.3.3 Advantages and Disadvantages of Boronizing

Table 2.7 shows the advantages and disadvantages of using the boronizing as the process.

Table 2.7: Advantages and disadvantages of boronizing process

(Source: Thallesthadeu, 2014)

Advantages	Disadvantages
High hardness and wear resistance retained in elevated temperatures	Process is inflexible and labor intensive
Enhance chemical corrosion resistance against acids and molten metals	The conventional thermochemical process for boriding is very slow
Lubricant surface that prevents the metal of aqueous corrosion	The partial removal of layer for tolerance is only did by an expensive method
Increased fatigue life	It is most applied to components with a large cross sectional area

2.4 Microscopy

2.4.1 Optical Microscopy

Instruments to produce magnified visual or photographic images of small objects are called microscopes. Microscope is used to achieve the tasks such as produce the specimen magnified image, the details in the image must be separated, and to extract the details that are visible to the human eye or camera (Inc, 2012).

Optical instrument as in Figure 2.1 is the equipment that containing one or more lenses. Focal plane of the lens that where the object has been placed, will produce an enlarged image of the object. The resolution limit where the submicron particle approaches the wavelength of visible light is 400nm to 700nm (Inc, 2012).



Figure 2.1 Optical microscopy (Source: Inc, 2012)

2.4.2 Scanning Electron Microscopy (SEM)

The Scanning Electron Microscopy (SEM) is an instrument that made up of two main components. The two main components are electronic console and electron column. The electronic console is for instrument adjustments. The images that are captured by the SEM can be saved in digital format or printed directly (Dunlap et al., 1997).

As stated that the SEM major component are divided into two, these components are part of seven primary operational systems (Jeol, 2009). The seven primary operational systems are vacuum, beam generation, beam manipulation, beam interaction, detection, signal processing, and display and record as in Figure 2.2.

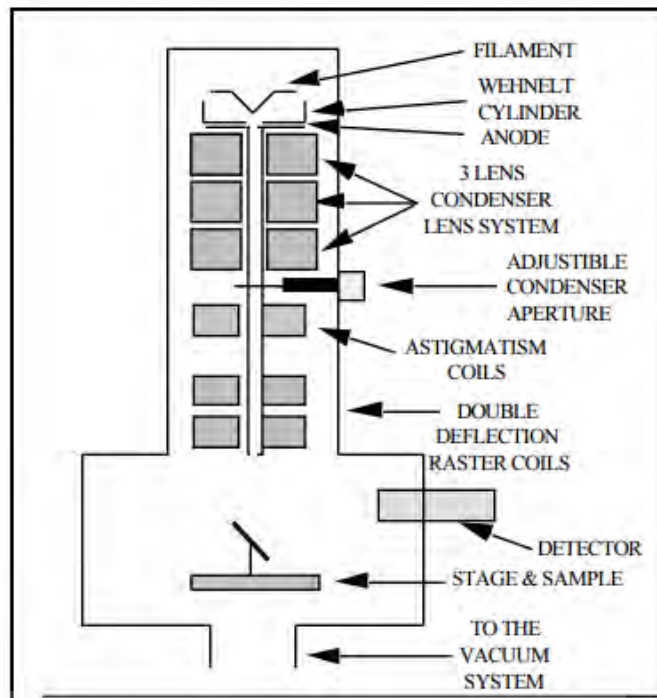


Figure 2.2 Diagram of SEM column and specimen chamber

(Source: Dunlap et al., 1997)

These systems are function together to determine the results and micrograph qualities such as magnification, resolution, field depth, contrast, and brightness (Dunlap et al., 1997).



2.5 Activation Energy

In chemistry, the minimum amount of energy that is required to activate atoms or molecules to a condition where they can undergo chemical conversion or physical transport is called activation energy. The typical characteristics of diffusion treatments are as in Table 2.8.

Process	Nature of case	Process temperature, °C (°F)	Typical case depth	Case hardness, HRC	Typical base metals	Process characteristics
Carburizing						
Pack	Diffused carbon	815–1090 (1500–2000)	125 μm –1.5 mm (5–60 mils)	50–63(a)	Low-carbon steels, low-carbon alloy steels	Low equipment costs, difficult to control case depth accurately
Gas	Diffused carbon	815–980 (1500–1800)	75 μm –1.5 mm (3–60 mils)	50–63(a)	Low-carbon steels, low-carbon alloy steels	Good control of case depth, suitable for continuous operation, good gas controls required, can be dangerous
Liquid	Diffused carbon and possibly nitrogen	815–980 (1500–1800)	50 μm –1.5 mm (2–60 mils)	50–65(a)	Low-carbon steels, low-carbon alloy steels	Faster than pack and gas processes, can pose salt disposal problem, salt baths require frequent maintenance
Vacuum	Diffused carbon	815–1090 (1500–2000)	75 μm –1.5 mm (3–60 mils)	50–63(a)	Low-carbon steels, low-carbon alloy steels	Excellent process control, bright parts, faster than gas carburizing, high equipment costs
Nitriding						
Gas	Diffused nitrogen, nitrogen compounds	480–590 (900–1100)	125 μm –0.75 mm (5–30 mils)	50–70	Alloy steels, nitriding steels, stainless steels	Hardest cases from nitriding steels, quenching not required, low distortion, process is slow, is usually a batch process
Salt	Diffused nitrogen, nitrogen compounds	510–565 (950–1050)	2.5 μm –0.75 mm (0.1–30 mils)	50–70	Most ferrous metals including cast irons	Usually used for thin hard cases <25 μm (1 mil), no white layer, most are proprietary processes
Ion	Diffused nitrogen, nitrogen compounds	340–565 (650–1050)	75 μm –0.75 mm (3–30 mils)	50–70	Alloy steels, nitriding steels, stainless steels	Faster than gas nitriding, no white layer, high equipment costs, close case control
Carbonitriding						
Gas	Diffused carbon and nitrogen	760–870 (1400–1600)	75 μm –0.75 mm (3–30 mils)	50–65(a)	Low-carbon steels, low-carbon alloy steels, stainless steel	Lower temperature than carburizing (less distortion), slightly harder case than carburizing, gas control critical
Liquid (cyaniding)	Diffused carbon and nitrogen	760–870 (1400–1600)	2.5–125 μm (0.1–5 mils)	50–65(a)	Low-carbon steels	Good for thin cases on noncritical parts, batch process, salt disposal problems
Ferritic nitrocarburizing	Diffused carbon and nitrogen	565–675 (1050–1250)	2.5–25 μm (0.1–1 mil)	40–60(a)	Low-carbon steels	Low-distortion process for thin case on low-carbon steel, most processes are proprietary
Other						
Boriding	Diffused boron, boron compounds	400–1150 (750–2100)	12.5–50 μm (0.5–2 mils)	40–>70	Alloy steels, tool steels, cobalt and nickel alloys	Produces a hard compound layer, mostly applied over hardened tool steels, high process temperature can cause distortion
Thermal diffusion process	Diffused carbide layers via salt bath processing	800–1250°C (1475–2285 °F)	2–20 μm (0.08–0.8 mil)	>70	Tool steels, alloy steels, medium-carbon steels	Produces a hard compound layer, mostly applied over hardened tool steels, high process temperature can cause distortion

(a) Requires quench from austenitizing temperature

Table 2.8: Typical characteristics of diffusion treatments
(Source: Davis, 2002)

Meanwhile, the transition state theory mentioned that the difference in energy content between atoms or molecules in an activated or transition-state configuration and the corresponding atoms and molecules in their initial configuration is the activation energy. The diffusion coefficient is as below, (Encyclopædia, 2015)

$$D = D_0 e^{\left(\frac{-E_a}{RT}\right)} \quad (2.1)$$

Where,

D = growth rate constant

E_a = activation energy (J/mol)

R = gas constant (J/mol K)

T = temperature in Kelvin (K)

D_0 = pre-exponential constant

e = exponential

2.5.1 Arrhenius Equation

An equation that display the effect of changes of temperature on the rate constant and thus on the rate of reaction or the amount of energy required to ensure that a reaction happens is the Arrhenius Equation. At the high temperature, the probability of two molecules will collide is higher. It can be concluded that the boride layer thickness can be described by a power function for process times. The E_a is the symbol in mathematical expressions for activation energy. It usually represented by the reaction rate constant, (LibreTexts et al., 2013)

$$k = A e^{\left(\frac{-E_a}{RT}\right)} \quad (2.2)$$

Where,

k = rate constant

E_a = activation energy (J/mol)

R = gas constant (J/mol K)

T = temperature in Kelvin (K)

A = pre-exponential constant

CHAPTER 3

METHODOLOGY

3.1 Introduction

In this chapter, the topic that will be discussed is about the method that will be used in this study. The aid from the Flow chart as in Appendix A and Gantt chart are being used as the guideline to complete this study. For this project, it starts with the material selection for the specimen until the material characterization process in order to get the structure of the specimen and thus to calculate the Arrhenius Equation.



اونيورسيتي تيكنيكل ماليسيا ملاك

UNIVERSITI TEKNIKAL MALAYSIA MELAKA

3.3 Material

Material used as the specimen is mild steel. Mild steel have a good balance of toughness, strength and ductility. For surface preparation, the chemical composition, rolling and heating processes used specific manufacturing controls. The mild steel is suitable to fabrication processes such as welding, drilling, machining, and heat treating. Figure 3.2 shows the mild steel that been use as the material for this project.



Figure 3.2 Mild steel

3.4 Specimens

3.4.1 Design of specimen

After the material has been selected then the design processes begin. For designing the specimen, AutoCAD Software has been used. In this study, the designed specimen should suit with and can be inserted in the available container. The design for the cornered surface is as shown in Figure 3.3 (a) and Figure 3.3 (b). The dimension of the design is 20mm for each length, width and height. There are four cornered shapes for the specimen such as 1mm fillet, 90° sharp cornered, 5mm radius corner and chamfer.

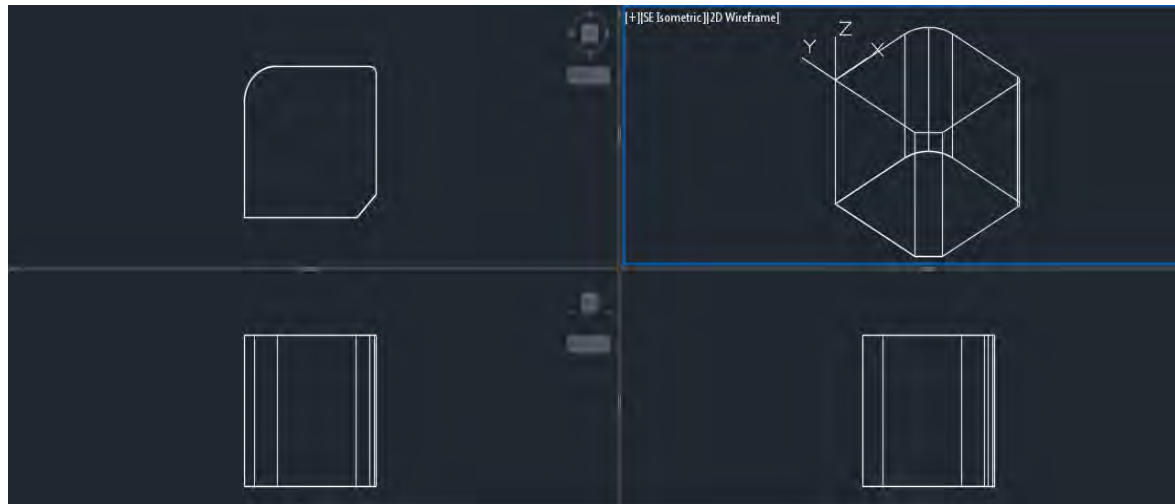


Figure 3.3 (a) Design of cornered surface specimen

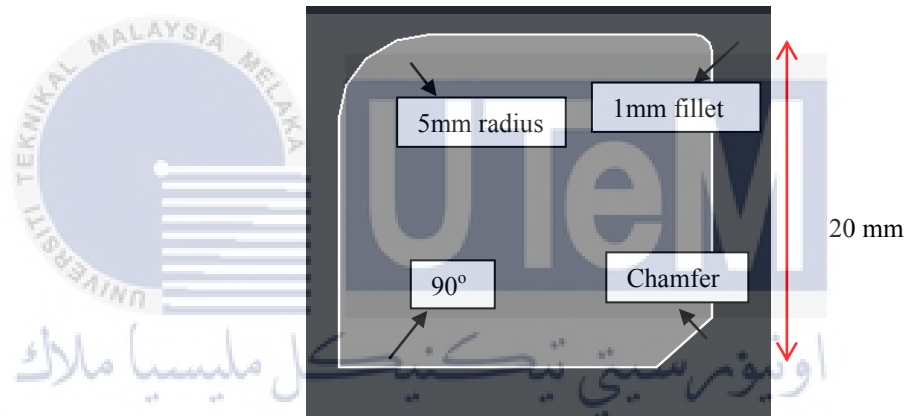


Figure 3.3 (b) Top view of the design

3.4.2 Fabrication

The fabrication process is the process where the material will be shaped according to the geometry that has been designed. In this fabrication process, it will be divided into three main processes that are

1) Cutting

From the long mild steel bar as in Figure 3.1, the steel was cut into 30mm for 9 pieces by using the bandsaw machine as in Figure 3.4 (a), Figure 3.4 (b) and Figure 3.5 is the steel block that have been cut.



Figure 3.4 (a) Bandsaw machine

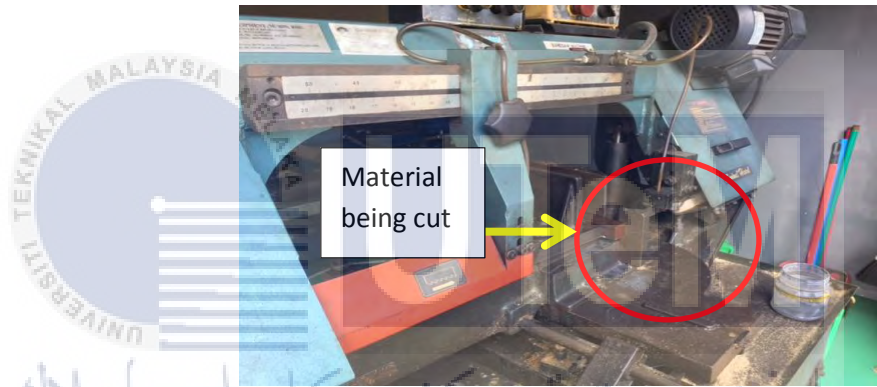


Figure 3.4 (b) Cutting materials using bandsaw machine

UNIVERSITI TEKNIKAL MALAYSIA MELAKA

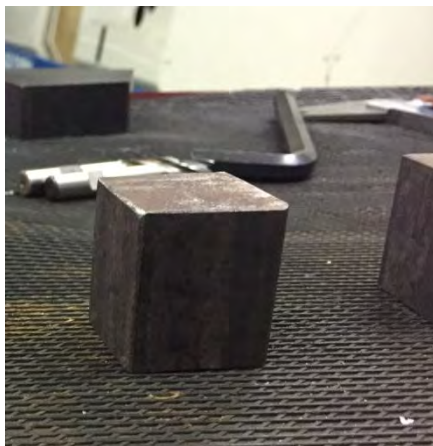


Figure 3.5 Steel block

Cutting process includes cutting the specimen after the fabrication using CNC milling process. The specimen to be cut is as in Figure 3.6. The specimens have to be cut manually using handsaw because the specimen is small and the bandsaw machine cannot be used.

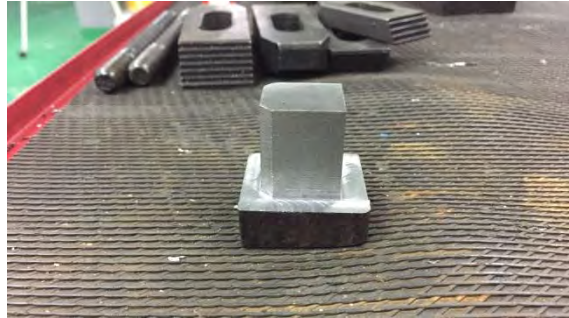


Figure 3.6 Material to be cut using handsaw

2) Milling

After the specimens have been cut by using the handsaw machine, the next step is using CNC milling machine as in Figure 3.7. The CNC machine is using coding to do the work. The selection of cutting tools must be suitable with the finishing specimen that needed and the cutting tools come in a range of sizes, materials, and geometry types. During the CNC milling process, the door must be closed for safety feature. Figure 3.8 shows the specimen before and after CNC milling machine process.



Figure 3.7 CNC milling machine

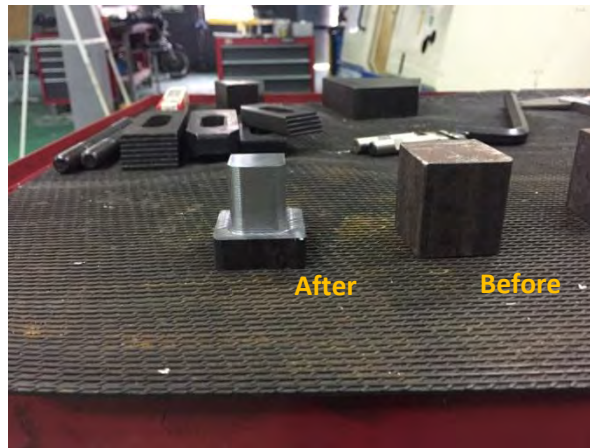


Figure 3.8 Specimen before and after CNC milling machine process

3) Grinding

The last processes for fabrications are grinding the edge surface of the specimen by using the grinder. This process is important in order to eliminate the sharp and extra chips at the edge of surface. Besides that, grinding process also helps to create a flat surface at the top surface of the specimen as in Figure 3.9.

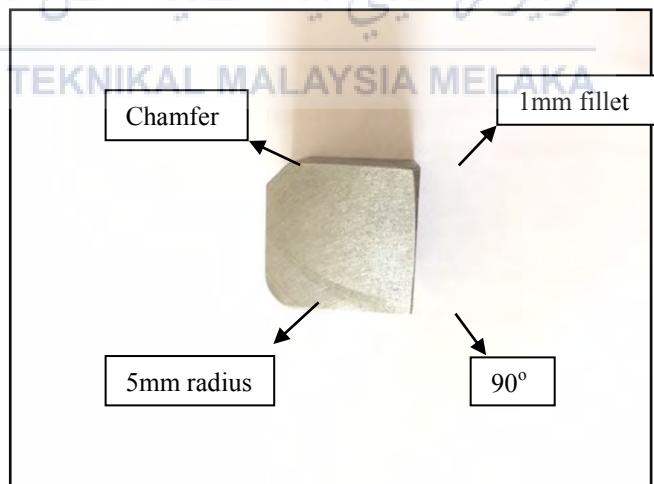


Figure 3.9 Finishing surface after grinding

3.5 Boronizing Process

3.5.1 Preparation

There are many types of boronizing treatment and for this study; the powdered boronizing will be used because it is easy to conduct and low cost process. Before the boronizing processes begin, the specimen must be cleaned using the acetone and let it dry. This is to remove unwanted particle of the surface of the specimen. After the specimens dry, than it will be placed in the container. Figure 3.10 (a) shows how the boronizing powders are filled up in the container. The specimens for this study have been placed in the center of the container as in Figure 3.10 (b) and filled the container with the boronizing powder at all sides and covered with a lid. The schematic diagram for the preparation for boronizing as in Figure 3.10 (c)



Figure 3.10 (a) Fill up the boronizing powder in container
(Source: Avion, 2016)

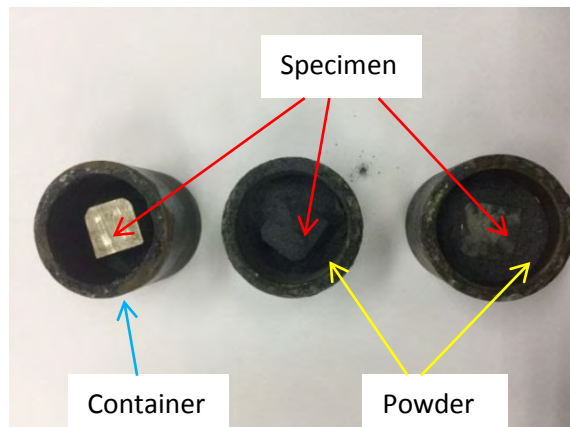


Figure 3.10 (b) Specimens in container with boronizing powders.

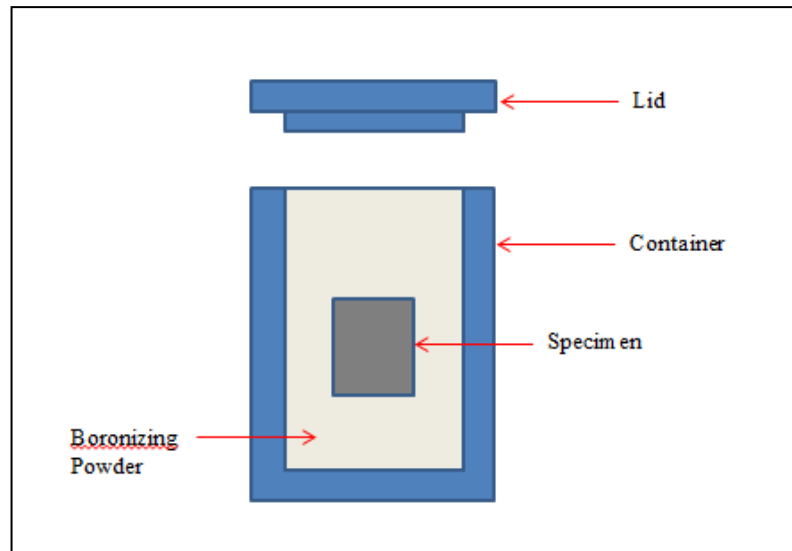


Figure 3.10 (c) Schematic diagrams for boronizing preparation

3.5.2 Process

In this study, the furnace will be used in order to complete the boronizing process as in Figure 3.11 (a) and (b) Figure 3.12 shows the hot container with the specimens were removed from furnace. The schematic diagram of the boronizing process is as Figure 3.13.



Figure 3.11 (a) Furnace



Figure 3.11 (b) Furnace



Figure 3.12 Hot container removed from furnace

UNIVERSITI TEKNIKAL MALAYSIA MELAKA

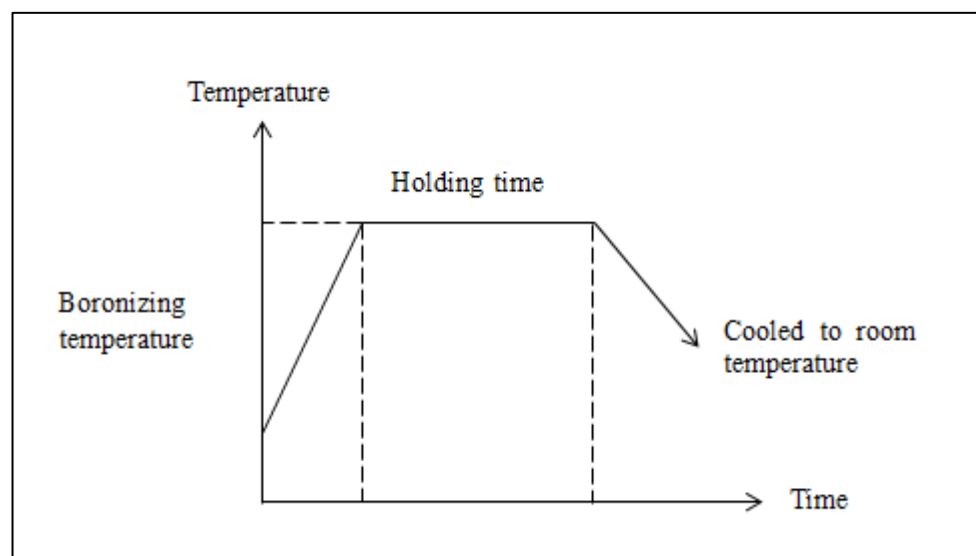


Figure 3.13 Schematic diagram of boronizing process

For the boronizing process, it held at three different temperature and duration that are 850°, 900°, 950° and in 2, 4 and 6 hours, respectively. The temperature and time were the factor that affecting the diffusion reaction. The diffusion reactions take place in between the boron layer and the specimen. The process of boronizing was repeated twice for respective time and temperature to get the average of boride layer thickness.

The container was placed in the furnace that has been heated at desired temperature and time. After the process has reached the desired time, the containers were taken out and cooled at room temperature. The specimens were removed from the container and used for material characterization method.

3.6 Material Characterization

To view the microstructure of specimen or material, material characterization is needed to create a proper viewing for it. There are several steps for material characterization process such as

i. Mount

Where the specimens being compress and heating by bakelite powder. This is to form solid disk so that it can be used to handle the sample.

ii. Grind

Process that function as to cut small chip at the surface of the specimen as in Figure 3.14.

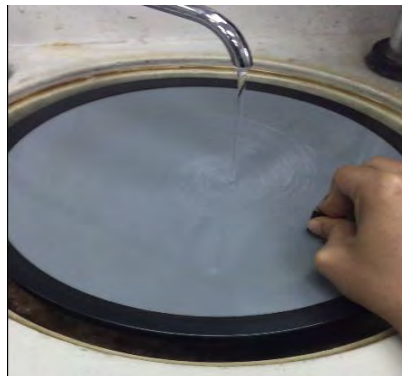


Figure 3.14 Grinding specimen

iii. Polish

Polishing in order to ensure the finishing surfaces are smooth.

iv. Etching

Process where the etching agent is etches at the specimen to show clearer view of the grain structure.

v. Microscope

A device used to observe the microstructure of specimen before using the SEM as in Figure 3.15 below.



Figure 3.15 Optical microscope

Figure 3.16 the basic steps for specimen preparation-microscopy (Mukhopadhyay, 2003).

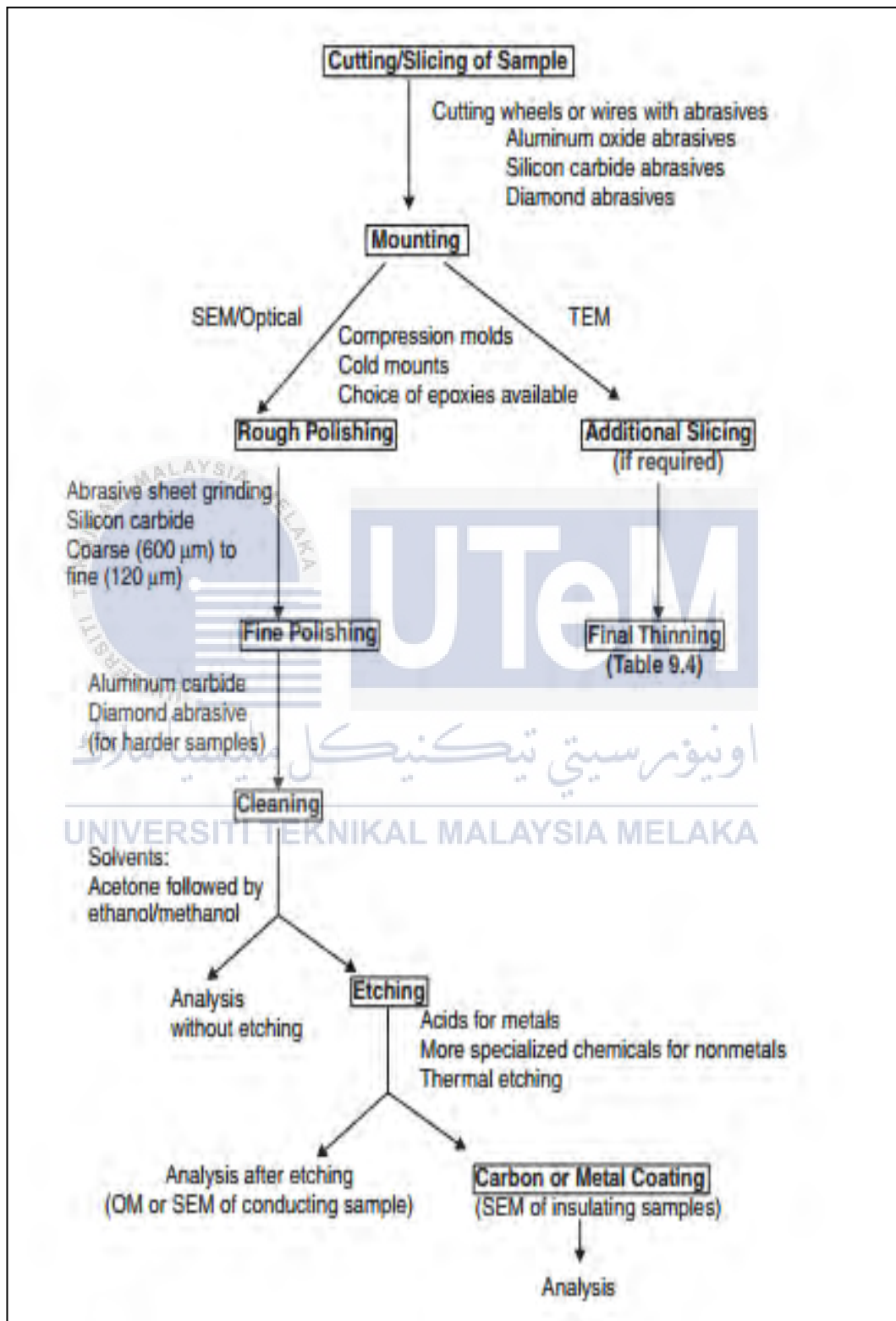


Figure 3.16 Basic steps for specimen preparation-microscopy (Source: Mukhopadhyay, 2003).

3.7 Activation Energy

One of the most important factors affecting the rate of a reaction is the activation energy, E_a . The Fick's first law of diffusion is as Eq (3.1) (Çulha, 2006).

$$J = -D \cdot \frac{dc(x)}{dx} \quad (3.1)$$

Where the units are as

$$D = \text{cm}^2 / \text{sec}$$

$$J = \text{number}/\text{cm}^2 / \text{sec}$$

Fick's first law usually applies to steady state systems. This is where the concentration keeps constant. However, in many cases of diffusion, the concentration changes with time. The total thickness of the boride layer growth can be calculated as Eq (3.2) (Çulha, 2006).

$$d^2 = K t \quad (3.2)$$

Where,

d = the depth of boride layer

K = growth rate constant

t = temperature

3.7.1 Arrhenius Equation

The rate constant of a reaction depends on E_a is the Arrhenius Equation. Since Eq (2) (Çulha, 2006),

$$k = A e^{\left(\frac{-E_a}{RT}\right)} \quad (2.2)$$

Then

$$\ln k = \ln A e^{\left(\frac{-E_a}{RT}\right)} \quad (3.3)$$

In mathematical concept, it is known as the property of,

$$\ln (ab) = \ln a + \ln b \quad (3.4)$$

Let, $a = A$, and $b = e^{\left(\frac{Ea}{RT}\right)}$

Then,

$$\ln k = \ln (A) + \ln \left(e^{\left(\frac{Ea}{RT}\right)}\right) \quad (3.5)$$

Mathematical property,

$$\ln (e^c) = c \quad (3.6)$$

Let,

$$c = \left(\frac{Ea}{RT}\right) \quad (3.7)$$

Then,

$$\ln k = \ln (A) - \left(\frac{Ea}{RT}\right) \quad (3.8)$$

Let,

$$\ln k_1 = \ln (A) - \left(\frac{Ea}{RT_1}\right) \text{ and } \ln k_2 = \ln (A) - \left(\frac{Ea}{RT_2}\right) \quad (3.9)$$

Rearrange,

$$E_a = -R \left[\frac{(\ln k_2 - \ln k_1)}{\left(\frac{1}{T_2} - \frac{1}{T_1}\right)} \right] \quad (3.10)$$

3.8 Preliminary Result

Based on the previous study, the graph of boride layer against the boronizing time will be as Figure 3.17. As for this study, the pattern of the graph should be similar with the graph at Figure 3.17 that are parabolic pattern. The graph can be obtained by using the Fick's Law Eq (3.2).

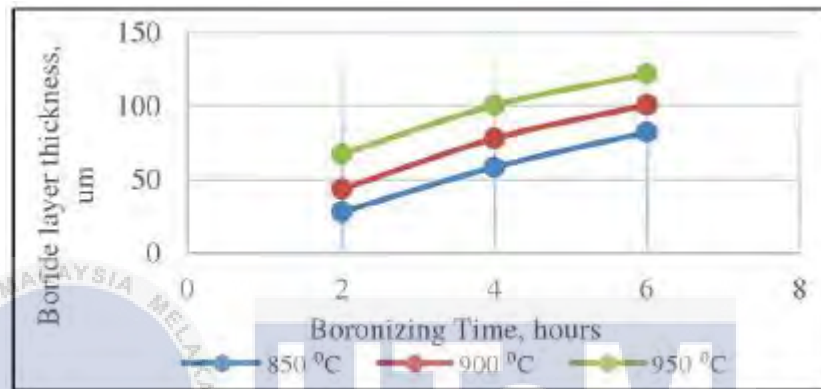


Figure 3.17 Boride layer against the boronizing time
(Source: Omar, 2016)

After the boronizing and material characterization process, the specimen will be analyzed to obtain the microstructure and thickness by using optical microscopic or SEM. Figure 3.18 below shows the example of the boride layer morphology and example of structure of steel after the boronizing process at 850° and 950° as in Figure 3.19 based on the previous study by using SEM.

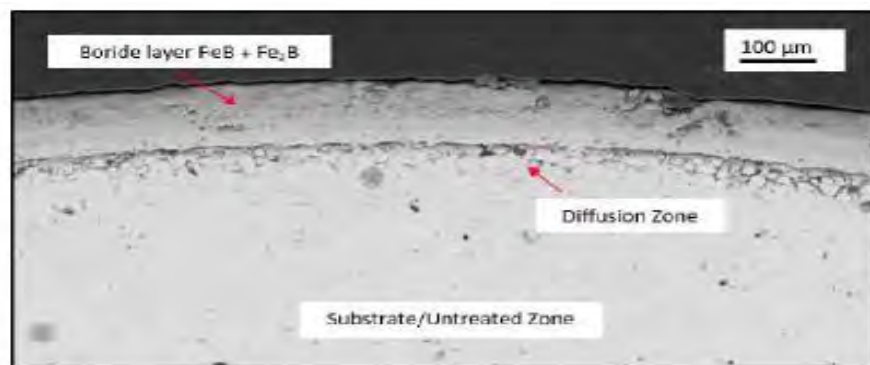


Figure 3.18 Boride layer morphology (Source: Omar, 2016).

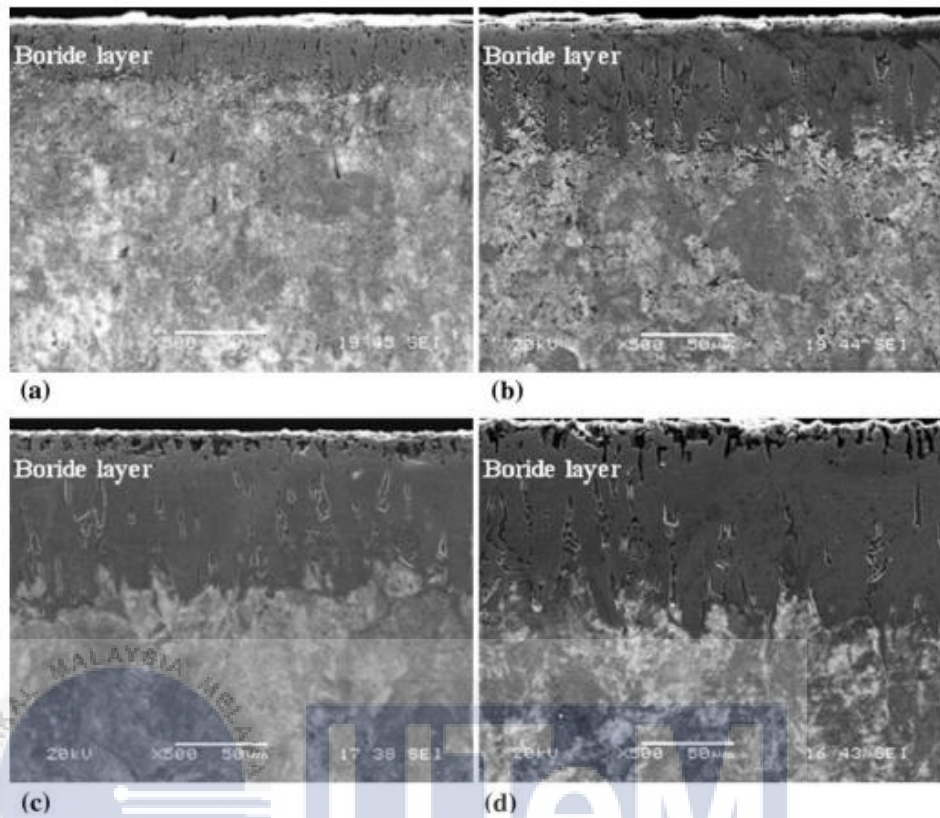


Figure 3.19 SEM micrographs of borided steel at 850 C for (a) 2 h, (b) 8 h and at 950 C for (c) 2 h, (d) 8 h (Source: Ipek et al, 2012)

CHAPTER 4

DATA AND RESULT

4.1 Introduction

In this chapter, there are eighteen specimens that have been experimented. The result of the boride layer thickness from the scanning electron microscope will be tabulated and analyzed. The processes and flow are as in Chapter 3. From the result, the activation energy will be calculated and discussed.

4.2 Microstructure

For this study, the boronizing process consists of total 19 specimens to be evaluated. The boride layer thickness needs to be determined in order to calculate the activation energy for the geometries. The boride layer thickness and micrographs for the geometries as shown in Figure 4.1 (a) 2Hour at 850 °C, (b) 4Hour at 850 °C , and (c) 6Hour at 850 °C, Figure 4.2 (a) 2Hour at 900 °C, (b) 4Hour at 900 °C , and (c) 6Hour at 900 °C, and Figure 4.3 (a) 2Hour at 950 °C, (b) 4Hour at 950 °C , and (c) 6Hour at 950 °C.

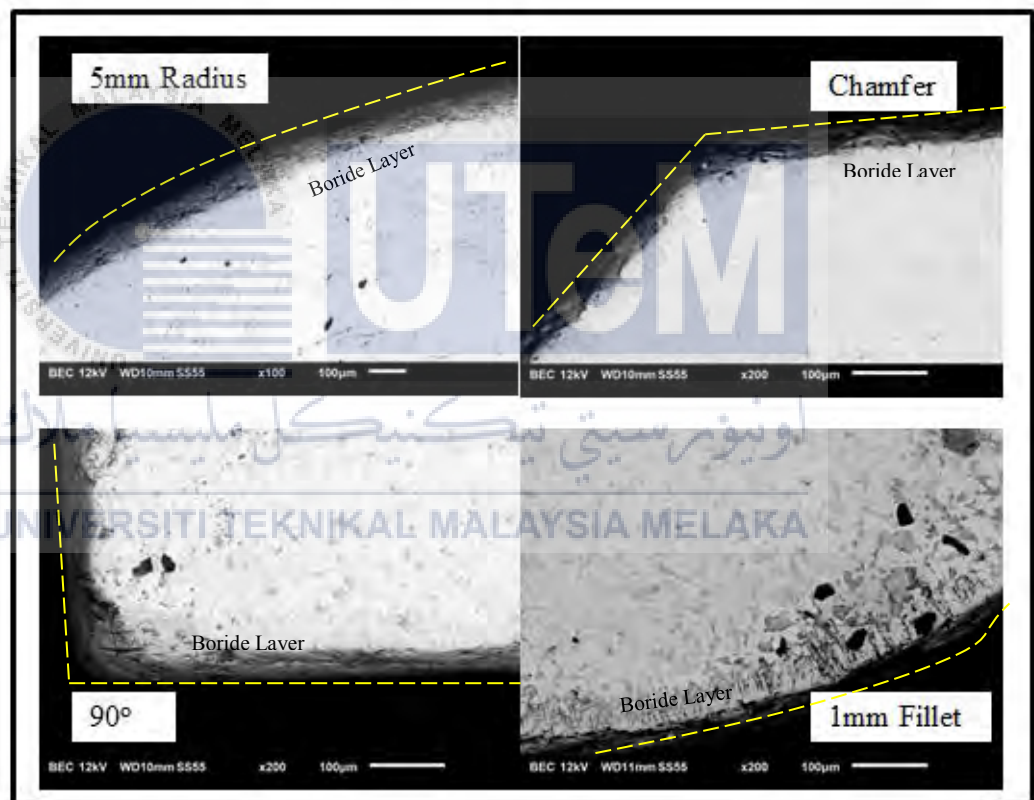


Figure 4.1 (a) Micrographs of the geometries for 2H at 850 °C

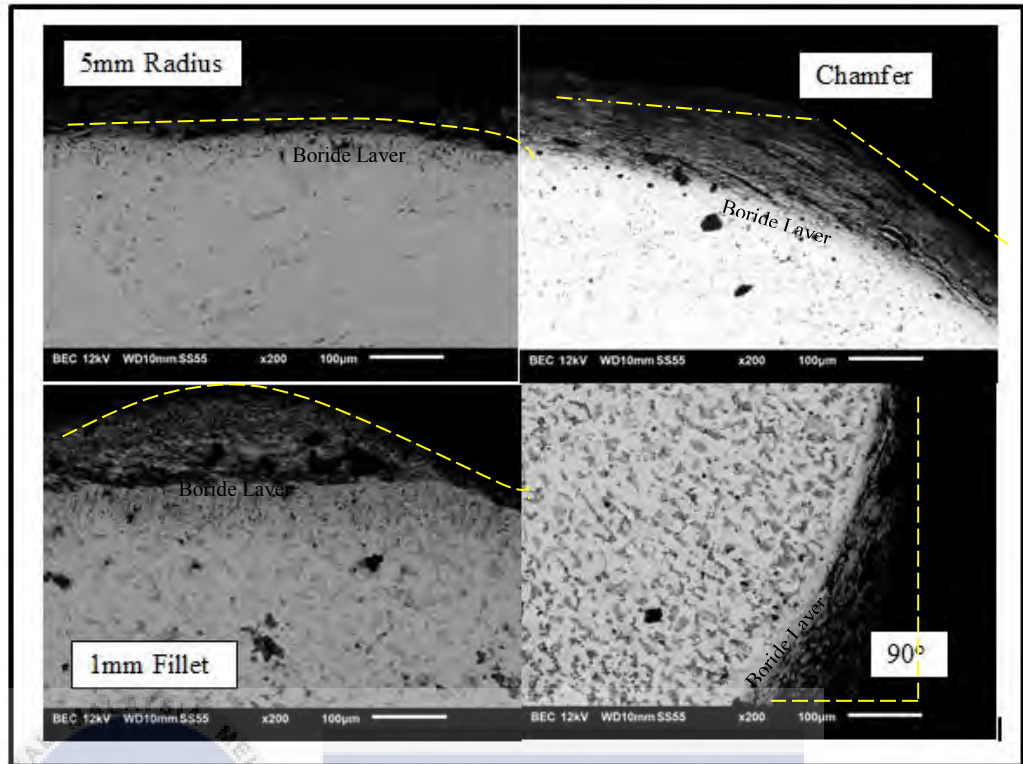


Figure 4.1 (b) Micrographs of the geometries for 4H at 850 °C

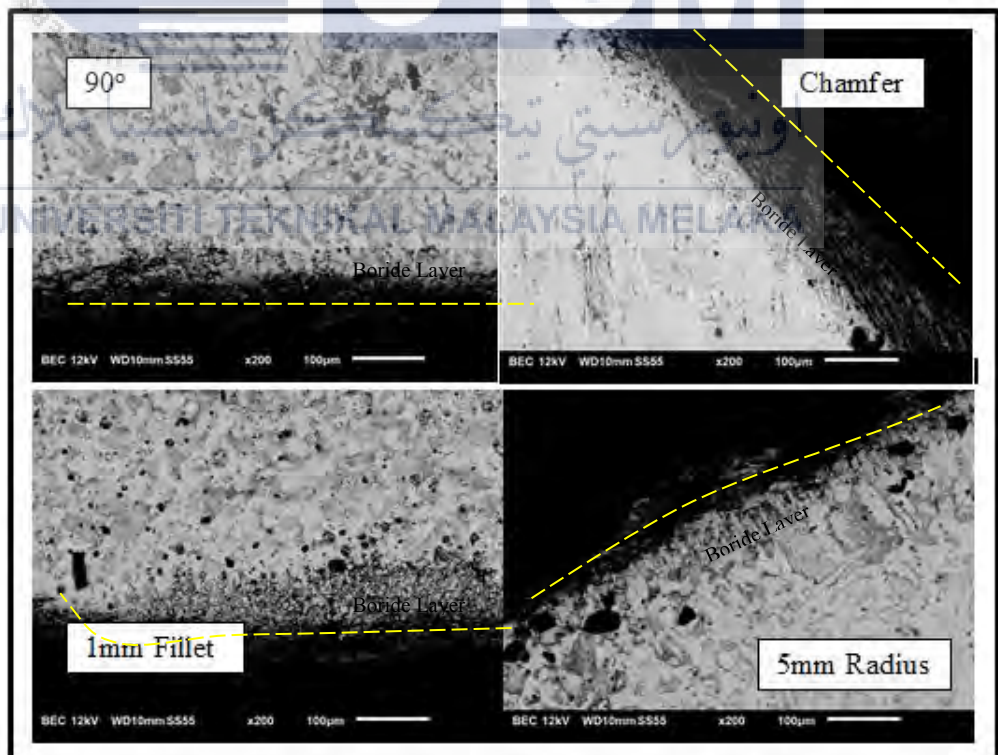


Figure 4.1 (c) Micrographs of the geometries for 6H at 850 °C

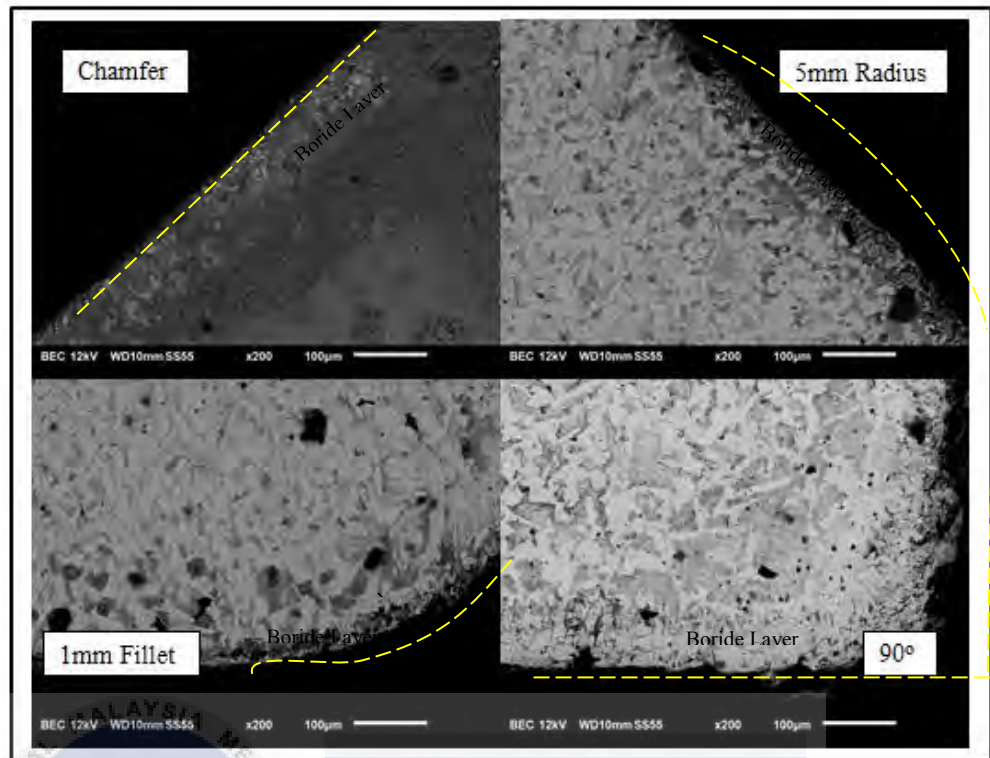


Figure 4.2 (a) Micrographs of the geometries for 2H at 900 °C

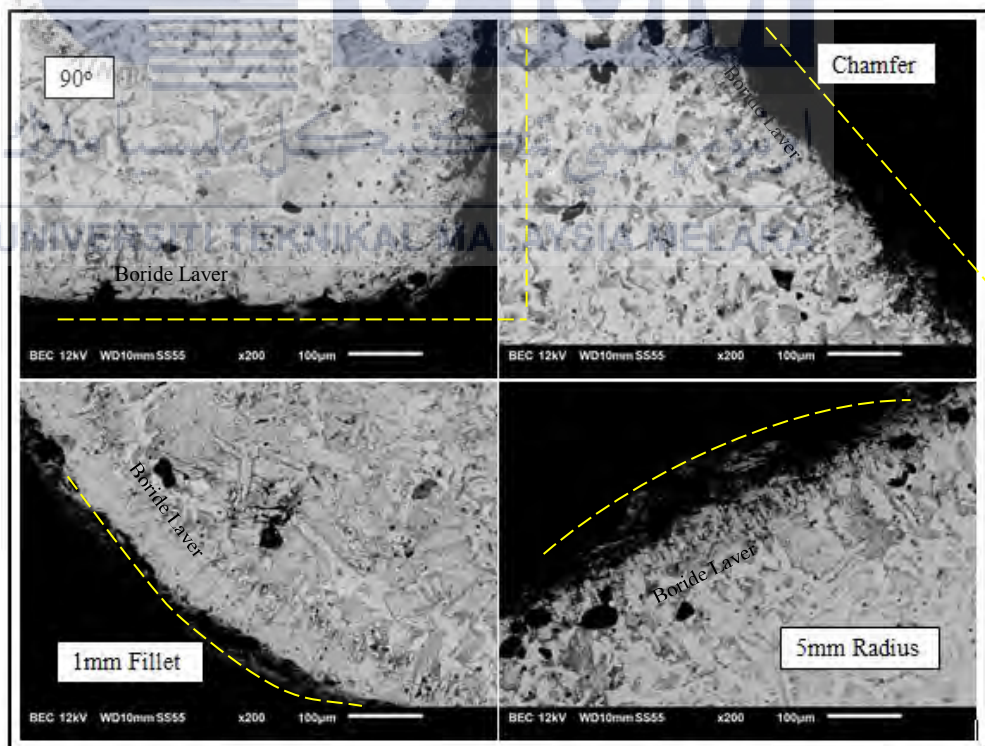


Figure 4.2 (b) Micrographs of the geometries for 4H at 900 °C

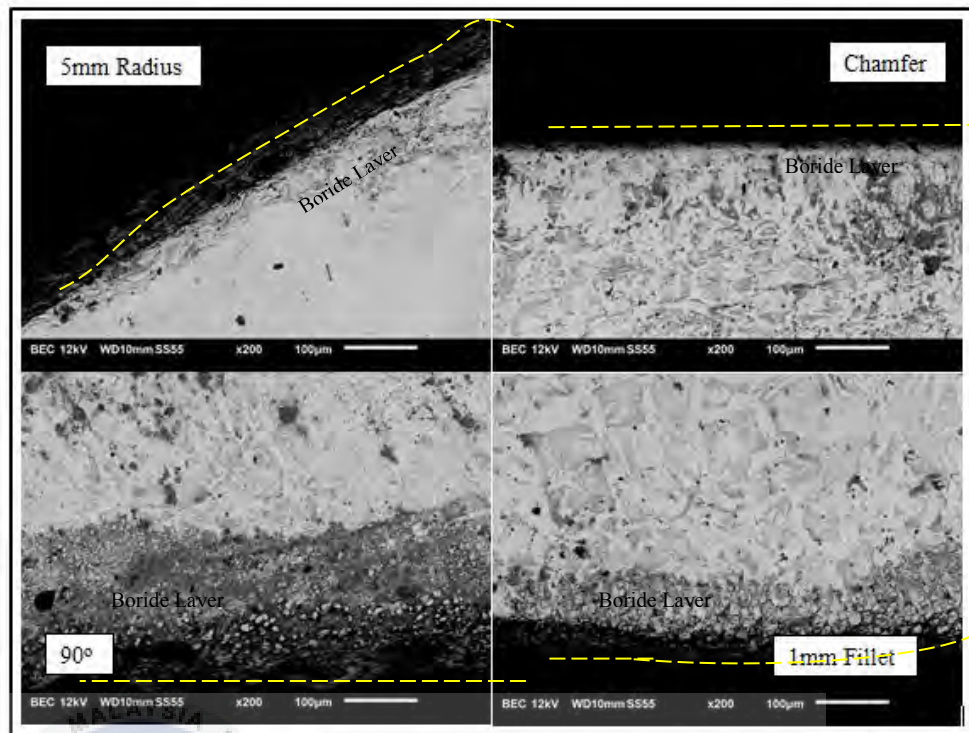


Figure 4.2 (c) Micrographs of the geometries for 6H at 900 °C

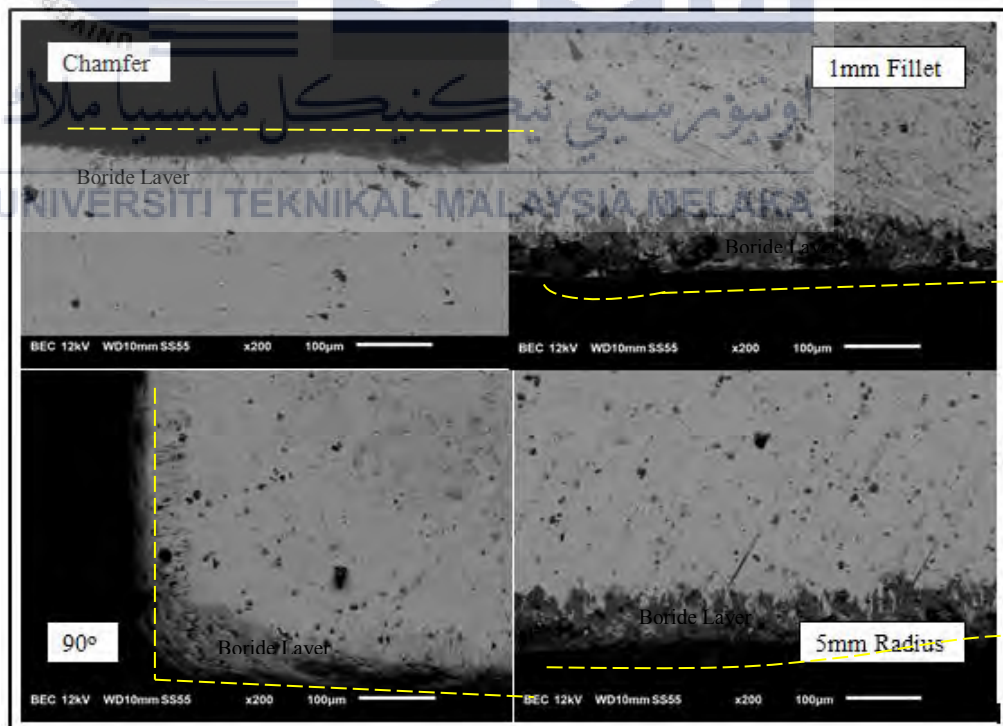


Figure 4.3 (a) Micrographs of the geometries for 2H at 950 °C

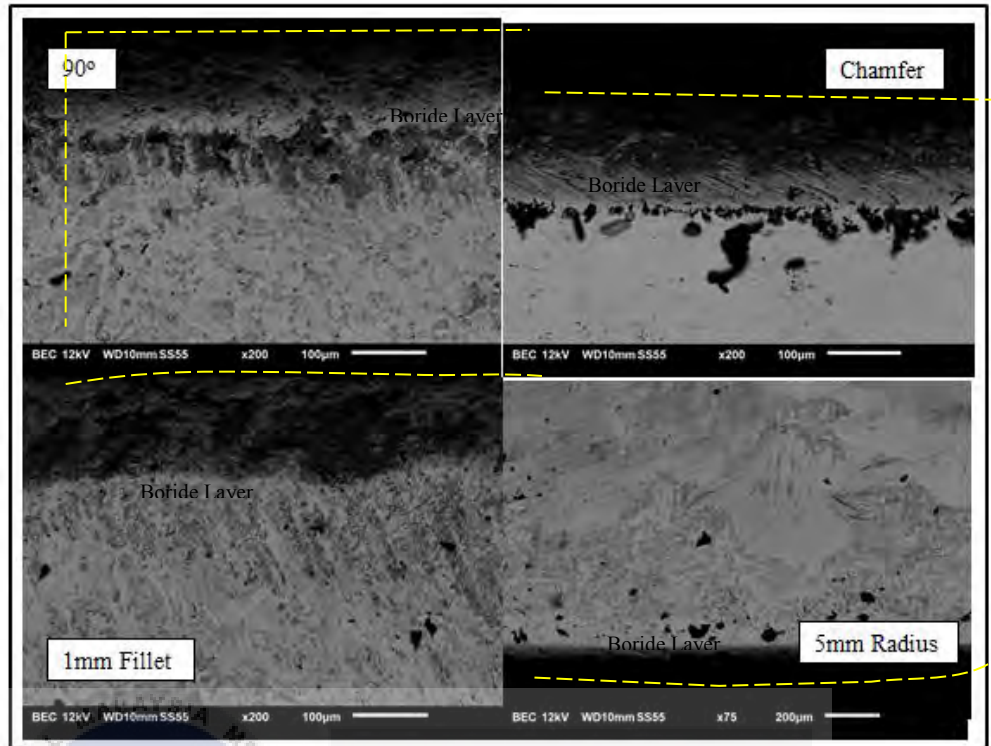


Figure 4.3 (b) Micrographs of the geometries for 4H at 950 °C

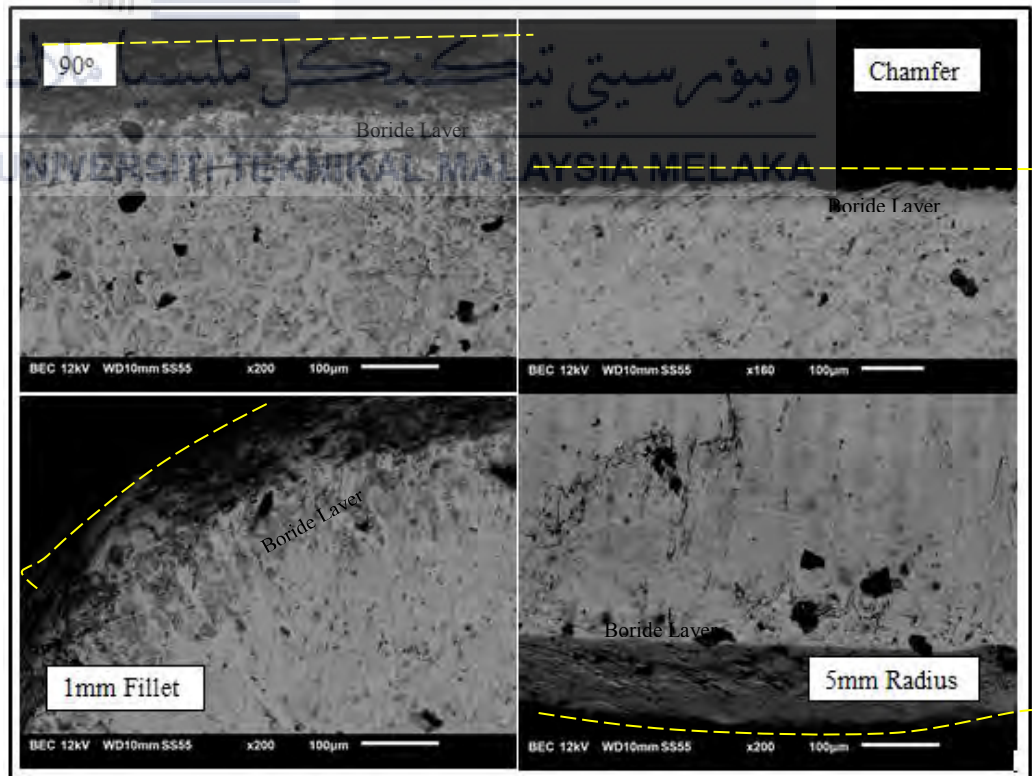


Figure 4.3 (c) Micrographs of the geometries for 6H at 950 °C

From the Figure 4.1, Figure 4.2 and Figure 4.3 it can be conclude that by using the SEM, the micrograph of the geometries shows the similar micrograph pattern from the previous study as in Figure 3.19 (Ipek et al, 2012) of Chapter 3, Methodology.

4.2.1 Data

The table 4.1 (a), (b), (c) and (d) are the results of the boride layer thickness for each of geometry after the material characterization method and by using the SEM to determine the thickness. It shows the temperature, time and the thickness of the boride layer for the geometry. The standard deviations for each of the geometries are as in Appendix C.

Table 4.1 (a) Thickness for 90° at cornered geometry

Temperatures (°C)	Time (Hour)								
	2			4			6		
	1	2	Average (μm)	1	2	Average (μm)	1	2	Average (μm)
850	61.772	54.841	58.307	40.287	88.011	64.129	49.358	80.689	65.024
900	72.385	45.981	59.183	86.783	45.587	66.185	109.342	30.215	69.779
950	69.728	52.110	60.919	84.513	49.258	66.886	90.179	53.002	71.591

Table 4.1 (b) Thickness for fillet cornered geometry

Temperatures (°C)	Time (Hour)								
	2			4			6		
	1	2	Average (μm)	1	2	Average (μm)	1	2	Average (μm)
850	50.293	26.82	38.557	54.653	36.710	45.682	62.848	30.268	46.558
900	32.160	51.243	41.702	81.051	30.268	55.660	81.489	34.211	57.85
950	76.87	35.216	56.043	111.669	40.412	76.041	117.836	45.145	81.491

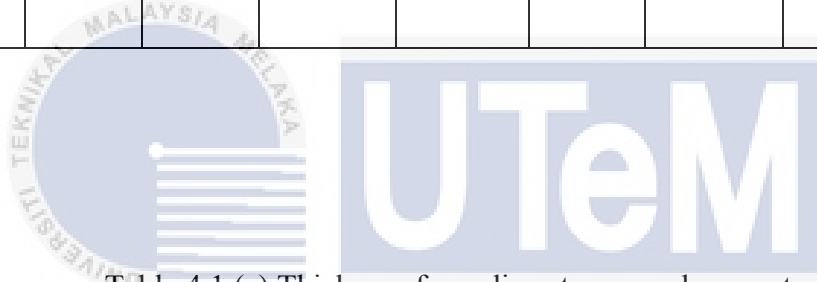


Table 4.1 (c) Thickness for radius at cornered geometry

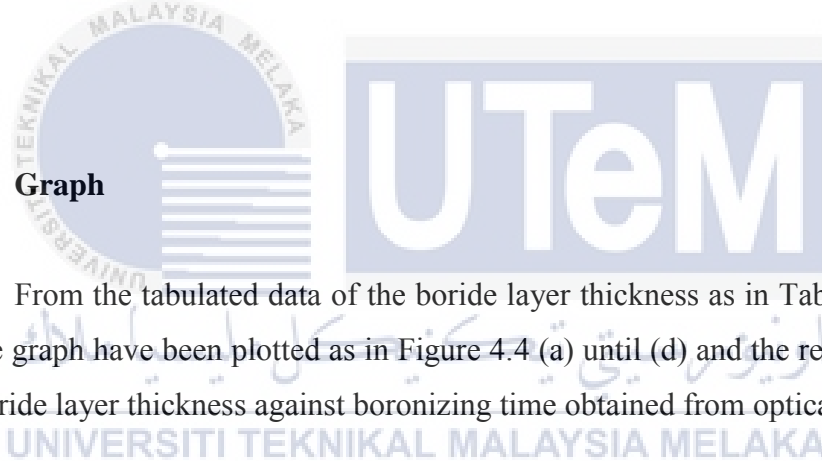
Temperatures (°C)	Time (Hour)								
	2			4			6		
	1	2	Average (μm)	1	2	Average (μm)	1	2	Average (μm)
850	60.126	44.573	52.350	28.008	78.215	53.112	71.246	45.125	58.186
900	36.568	73.158	54.863	52.542	75.157	63.850	46.971	81.547	64.259
950	75.683	48.113	61.898	128.476	30.015	79.246	43.701	117.317	80.509

Table 4.1(d) Thickness for chamfer cornered geometry

Temperatures (°C)	Time (Hour)								
	2			4			6		
	1	2	Average (μm)	1	2	Average (μm)	1	2	Average (μm)
850	82.515	48.660	65.588	45.019	88.171	66.595	38.142	97.287	67.715
900	45.38	83.851	65.616	70.65	63.512	67.081	60.504	98.802	79.653
950	54.504	87.023	70.764	57.334	89.641	73.488	74.592	101.211	87.902

4.2.2 Graph

From the tabulated data of the boride layer thickness as in Table 4.1 (a) until (d) the graph have been plotted as in Figure 4.4 (a) until (d) and the result shows that the boride layer thickness against boronizing time obtained from optical and SEM.



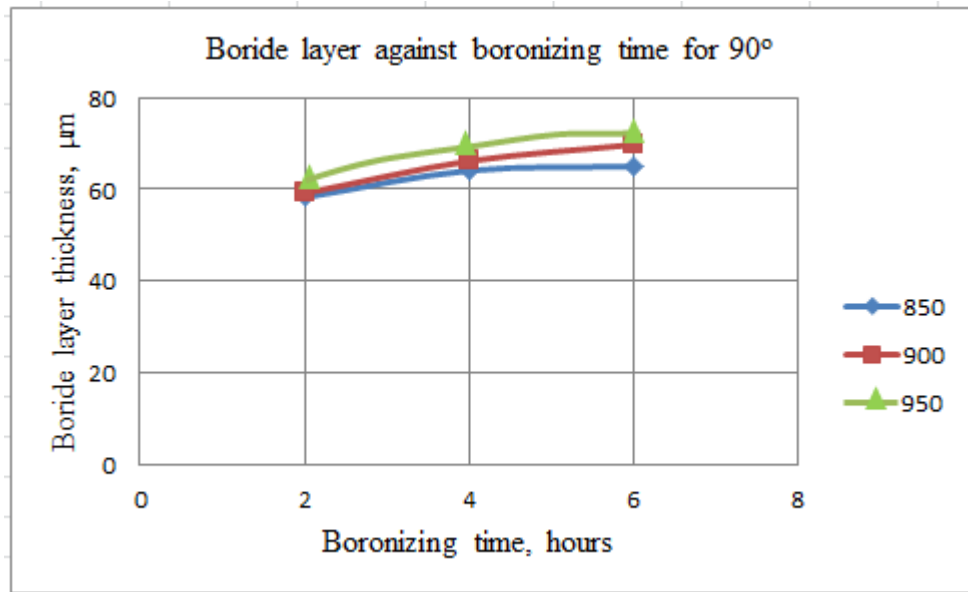


Figure 4.4(a) Graph of boride layers against boronizing time for 90°

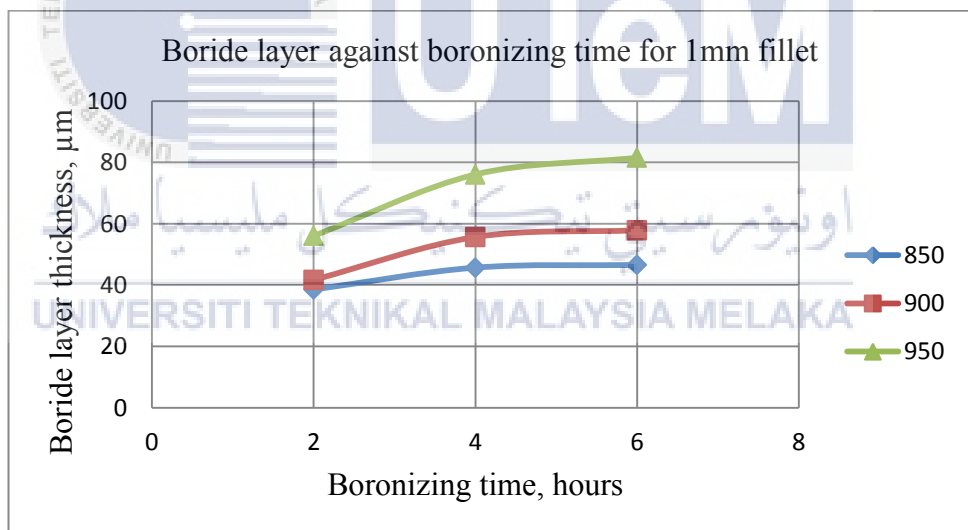


Figure 4.4 (b) Graph of boride layers against boronizing time for 1mm fillet

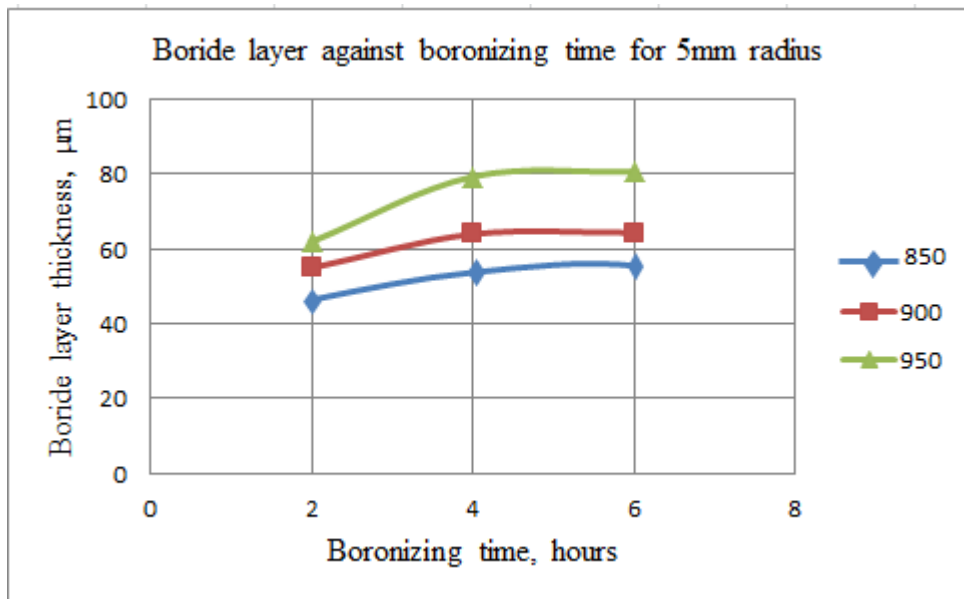


Figure 4.4 (c) Graph of boride layers against boronizing time for 5mm radius

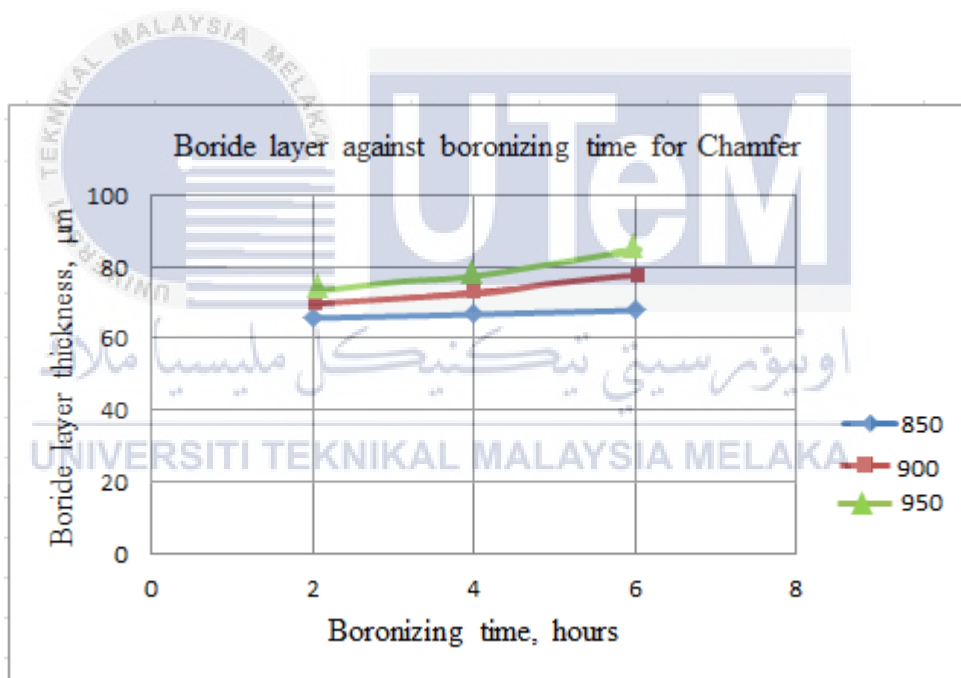


Figure 4.4(d) Graph of boride layers against boronizing time for chamfer

From the graph above, it shows that the most of the graph is parabolic pattern as shown previously in the Figure 3.17 (Omar, 2016) of Chapter 3, Methodology.

4.3 Kinetic Of Boron Diffusion

The kinetics of the layer growth is controlled perpendicularly into the substrate layer and can be describe as in Eq (3.2) and plotted as the square of boride layer thickness of borided carbon steel as a function of time.

4.3.1 90° Geometry

Table 4.2 (a) shows that the thickness data for the 90° and from the table, the squared boride layer against boronizing time is plotted as in Figure 4.5 (a). From the graph, the gradient can be obtained for each temperature and tabulated in Table 4.3 (a).

Table 4.2 (a) Thickness data for 90°

Temperature (K)	Time (Hour)		
	2	4	6
	Average (μm)	Average (μm)	Average (μm)
1123	3400	4113	4228
1173	3503	4380	4869
1223	3711	4474	5125

UNIVERSITI TEKNIKAL MALAYSIA MELAKA

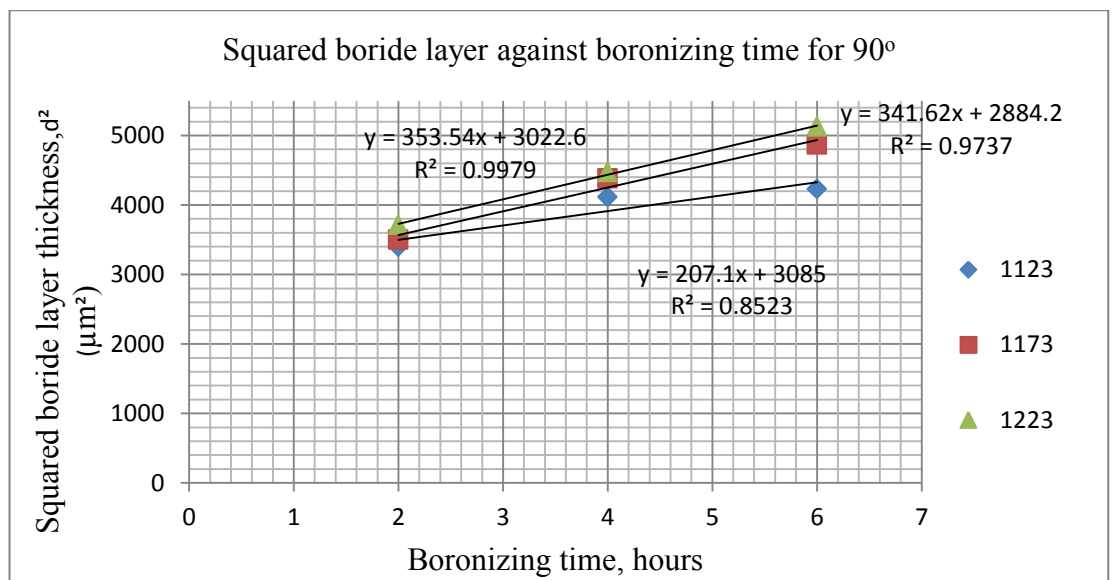


Figure 4.5 (a) Squared boride layer against boronizing time for 90°

Table 4.3 (a) Gradient of each temperature for 90°

Temperature ,T (K)	Gradient, k
1123	207.1
1173	341.62
1223	353.54

Table 4.4 (a) below shows the data that have been tabulated to plot the graph $\ln k$ versus $1/T$ as in Figure 4.6 (a). The gradient, k value was taken from the graph of Figure 4.5 (a).

Table 4.4 (a) Data of $\ln k$ and $1/T$ for 90°

Temperature ,1/ T (K ⁻¹)	Gradient, $\ln k$ (m ² /s)
0.000890	5.333
0.000853	5.834
0.000818	5.868

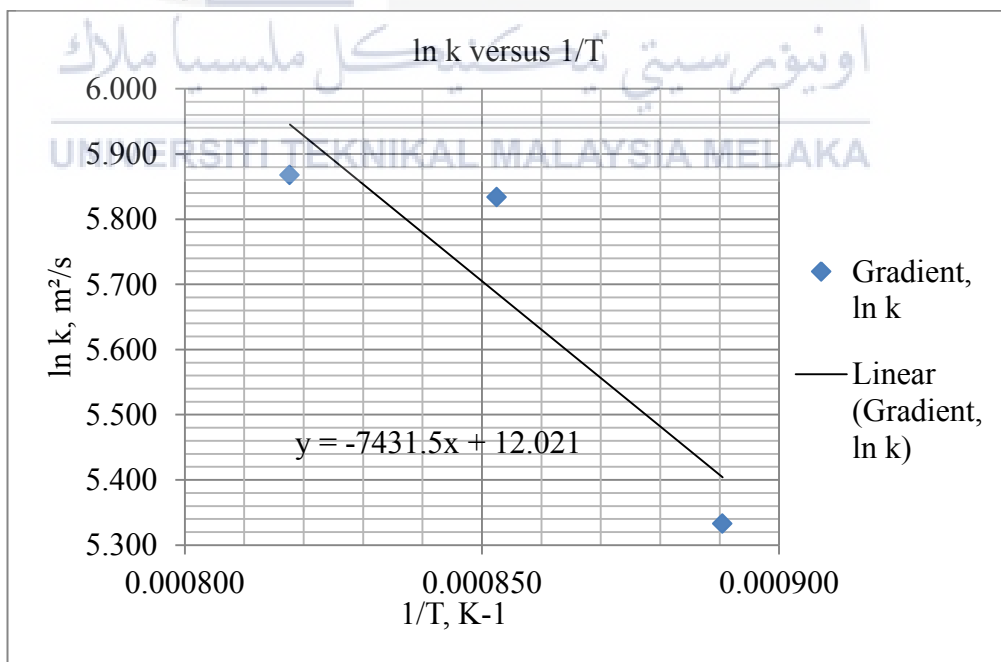


Figure 4.6 (a) Natural logarithm of growth rate constant ($\ln k$) as a function of reciprocal boronizing temperature ($1/T$) for 90°

From the Figure 4.6 (a) it shows that the gradient for the graph is -7431.5. In order to calculate the activation energy, the Eq (2.2) will be used.

4.3.2 1mm Fillet

From Table 4.2 (b) it shows that the thickness data for the 1mm fillet and from the data, the squared boride layer against boronizing time is plotted as in Figure 4.5 (b). The gradient can be obtained for each temperature from the graph and tabulated in Table 4.3 (b).

Table 4.2 (b) Thickness data for 1mm fillet

Temperature (K)	Time (Hour)		
	2	4	6
	Average (μm)	Average (μm)	Average (μm)
1123	1487	2087	2168
1173	1739	3098	3347
1223	3141	5782	6641

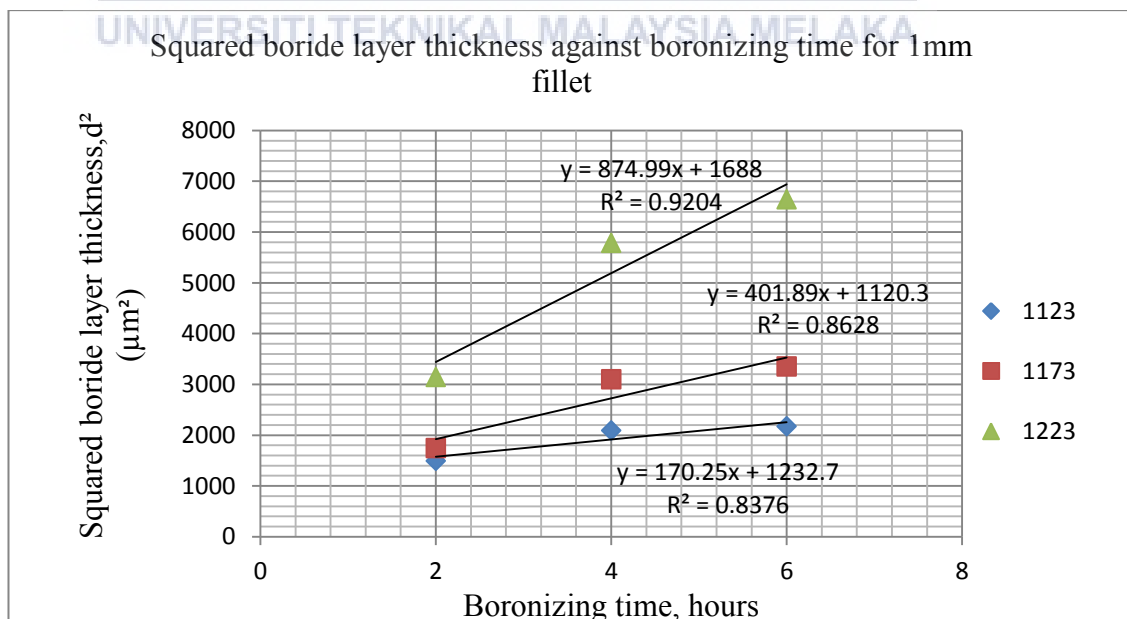


Figure 4.5 (b) Squared boride layers against boronizing time for fillet

Table 4.3 (b) Gradient of each temperature for 1mm fillet

Temperature, T (K)	Gradient, k
1123	170.25
1173	401.89
1223	874.99

Table 4.4 (b) shows the data that have been tabulated to plot the graph $\ln K$ versus $1/T$ as in Figure 4.6 (b). The gradient, k value was taken from the graph of Figure 4.5 (a).

Table 4.4 (b) Data of $\ln K$ and $1/T$ for 1mm fillet

Temperature, $1/T$ (K^{-1})	Gradient, $\ln k$ (m^2/s)
0.000890	5.137
0.000853	5.996
0.000818	6.774

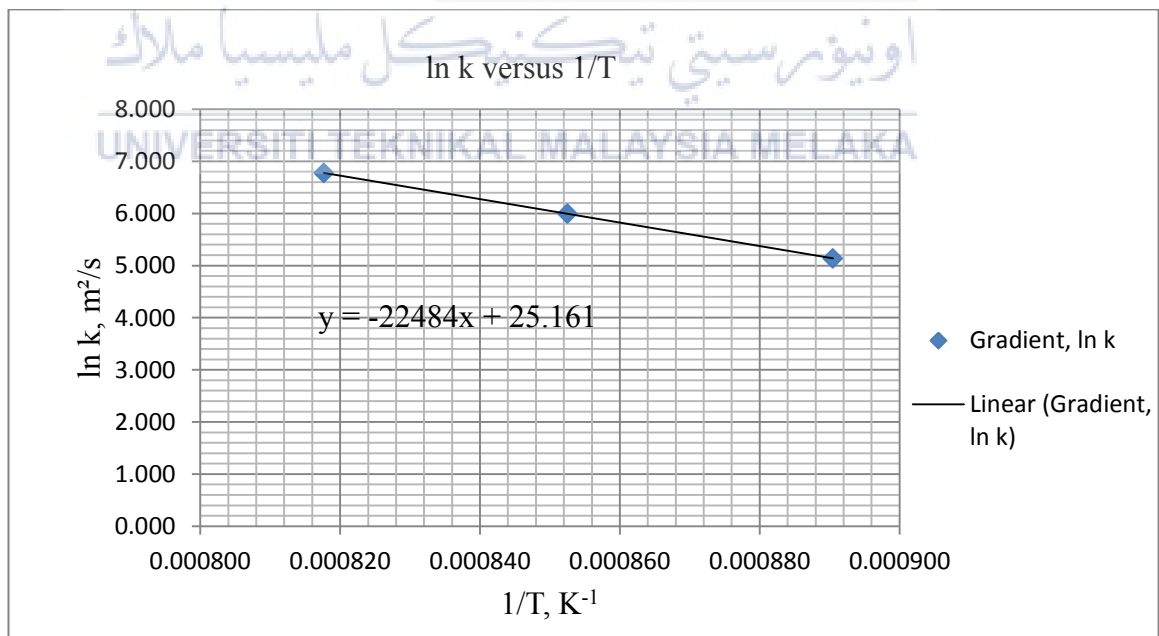


Figure 4.6 (b) Natural logarithm of growth rate constant ($\ln k$) as a function of reciprocal boronizing temperature ($1/T$) for 1mm fillet

From the Figure 4.6 (b) it shows that the gradient for the graph is -22484. In order to calculate the activation energy, the Eq (2.2) will be used.

4.3.3 5mm Radius

Table 4.2 (c) shows that the thickness data for the fillet and from the table below, the squared boride layer against boronizing time is plotted as in Figure 4.5 (c). The gradient can be obtained for each temperature from the graph and tabulated in Table 4.3 (c).

Table 4.2 (c) Thickness data for 5mm radius

Temperature (K)	Time (Hour)		
	2	4	6
	Average (μm)	Average (μm)	Average (μm)
1123	2741	2821	3386
1173	3010	4077	4129
1223	3831	6280	6482

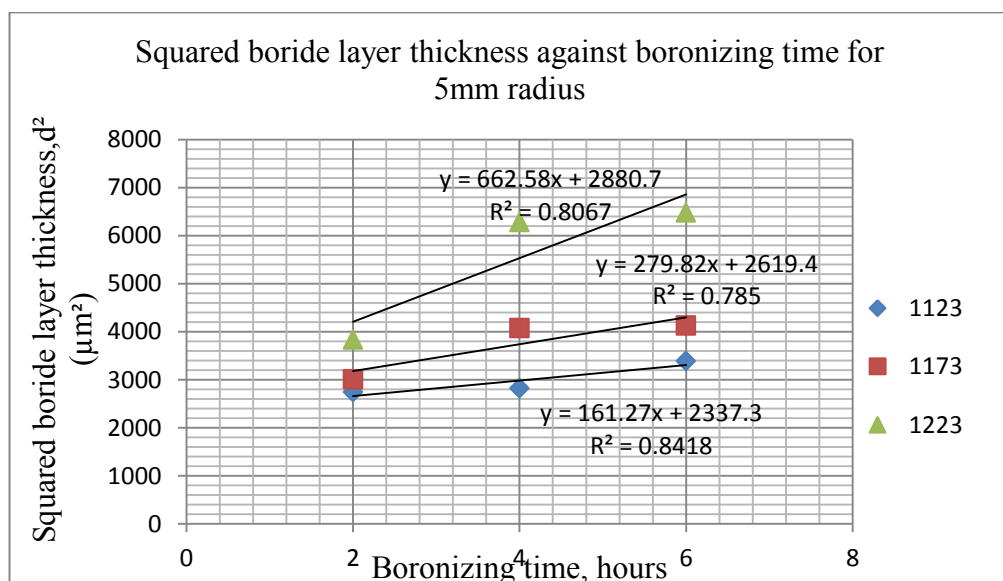


Figure 4.5 (c) Squared boride layers against boronizing time for 5mm radius

Table 4.3 (c) Gradient of each temperature for 5mm radius

Temperature ,T (K)	Gradient, k
1123	161.27
1173	279.82
1223	662.58

Table 4.4 (c) shows the data that have been tabulated to plot the graph $\ln k$ versus $1/T$ as in Figure 4.6 (c). The gradient, k value was taken from the graph of Figure 4.5 (c).

Table 4.4 (c) Data of $\ln k$ and $1/T$ for 5mm radius

Temperature ,1/ T (K ⁻¹)	Gradient $\ln k$ (m ² /s)
0.000890	5.083
0.000853	5.634
0.000818	6.496

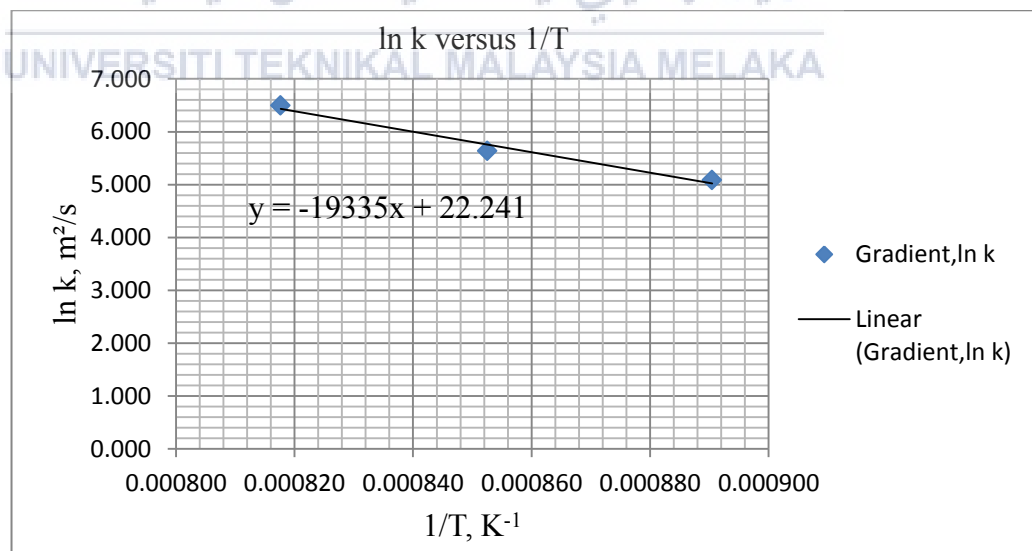


Figure 4.6 (c) Natural logarithm of growth rate constant ($\ln k$) as a function of reciprocal boronizing temperature ($1/T$) for 5mm radius

From the Figure 4.6 (c) it shows that the gradient for the graph is -19335. In order to calculate the activation energy, the Eq (2.2) will be used.

4.3.4 Chamfer

Based on the Table 4.2 (d), it shows that the thickness data for the fillet and from the table, the squared boride layer against boronizing time is plotted as in Figure 4.5 (d). The gradient can be obtained for each temperature from the graph and tabulated in Table 4.3 (d).

Table 4.2 (d) Thickness data for chamfer

Temperature (K)	Time (Hour)		
	2	4	6
	Average (μm)	Average (μm)	Average (μm)
1123	4302	4435	4585
1173	4305	4500	6345
1223	5008	5400	7727

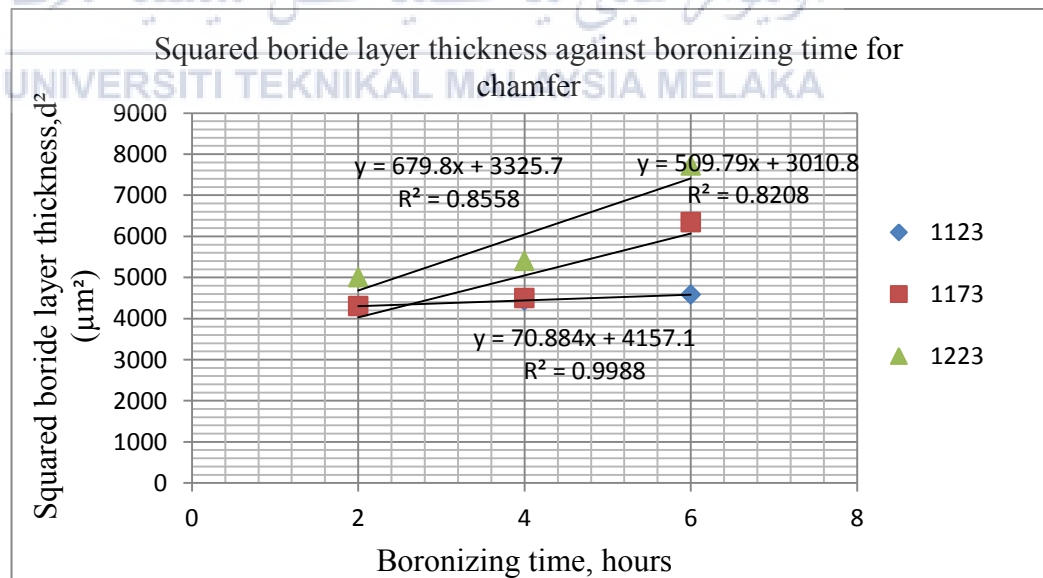


Figure 4.5 (d) Squared boride layer against boronizing time for chamfer

Table 4.3 (d) Gradient of each temperatures for chamfer

Temperature ,T	Gradient, k
1123	70.884
1173	509.79
1223	679.8

Table 4.4 (d) shows the data that have been tabulated to plot the graph $\ln K$ versus $1/T$ as in Figure 4.6 (d). The gradient, k value was taken from the graph of Figure 4.8 (d).

Table 4.4 (d) Data for $\ln K$ and $1/T$ for chamfer

Temperature ,1/ T	Gradient, $\ln k$ (m^2/s)
0.000890	4.261
0.000853	6.234
0.000818	6.522

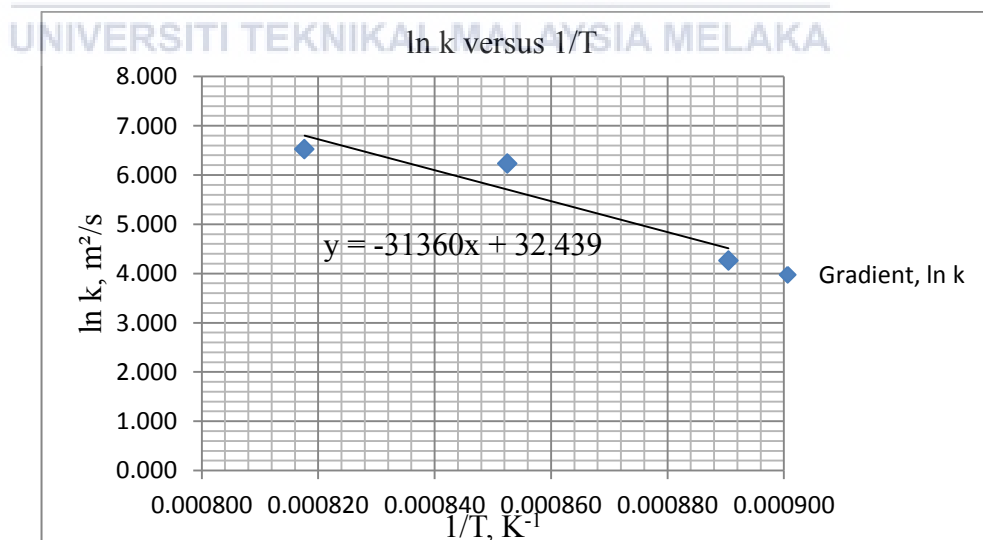


Figure 4.6(d) Natural logarithm of growth rate constant ($\ln k$) as a function of reciprocal boronizing temperature ($1/T$) for chamfer

From the Figure 4.6 (a) it shows that the gradient for the graph is -31360. In order to calculate the activation energy, the Eq (2.2) will be used.

4.4 Activation Energy

The plotted graph of $\ln K$ versus $1/T$ in Figure 4.9 (a), (b), (c), and (d) showed the linear relationship with the temperature and the value of activation energy measured from the slope using the Arrhenius Equation as in Eq (2.2).

$$k = Ae^{\left(\frac{-E_a}{RT}\right)} \quad (2.2)$$

The example of the calculation can be referred to Appendix B. Table 4.5 below shows that the result for the activation energy for geometries based on the gradient from \ln graph.

Table 4.5 Result for the activation energy for geometries

Geometry	Gradient, k	Activation energy, E_a (kJ/mol)
90°	-7431.5	61.785
Fillet	-22484	186.932
Radius	-19335	160.751
Chamfer	-31360	260.727

CHAPTER 5

DISCUSSION AND ANALYSIS

5.1 Introduction

In this chapter, the discussion and analysis will be discussed based on the data and result that have been recorded in the Chapter 4. The graph and result will be analysed to find which of the geometry that have the lowest activation energy thus the objective of this study can be achieved.



5.2 Microstructure Analysis

From the Figure 4.1 until Figure 4.3 (subsection 4.3), the micrograph of each geometries were taken by using the SEM. Before the microstructure can be seen clearly using the microscope and SEM, the surface of the specimen needs to be smooth without any scars. The specimen need to be grinded and polished until smooth then the specimens will be etched using the etching agent. After that, the boride layer can be seen using the microscope and the SEM.

Based on the result, it shows that from previous study as in Figure 3.19 (subsection 3.8) and this study, the micrographs have the similar pattern and it can be concluded that the boride layer formation is similar. The comparison can be seen as in the Figure 5.1 and Figure 5.2 below. The magnification of the micrograph is however, different. From the result of the micrographs, it shows that the micrograph have different length and thickness of the boride layer.

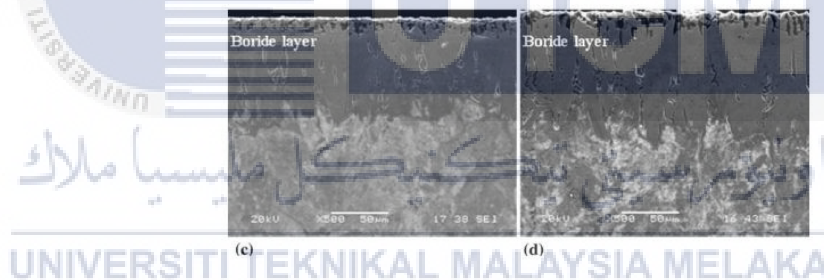


Figure 5.1 SEM micrographs of borided steel at 950 C for (c) 2 h, (d) 8 h

(Source: Ipek et al, 2012)

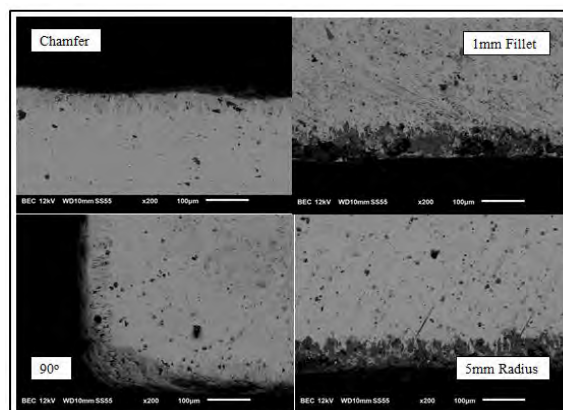


Figure 5.2 Micrographs of the geometries for 2H at 950 °C

5.3 Boride Layer Thickness Analysis

The boride layer thickness have been measured and tabulated as in the Table 4.1 (subsection 4.2.1) and from the tabulated data, the results shows an increased for each temperature and this has been proven as in the literature review on the background of boronizing. The thickness of boride layer will be increased as the temperature increased (Chegroune et al, 2016,).

The pattern of the graph shows that it has a parabolic pattern as in Figure 4.4 (subsection 4.2.2) and it is similar as in previous study. From the graphs, it shows that there are three lines that did not show the parabolic pattern that is from Figure 4.4 (d) for the chamfer geometry but the other nine lines shows the parabolic pattern. Even though the three lines from Figure 4.4 (a) not clearly shows the parabolic pattern but the thickness is increased as the temperature increased.

This is because of the reading for the thickness have a slightly increase and that cause the graph not in parabolic pattern and near to linear line graph pattern. Thus, it can be said that the boride layer thickness increases when the boronizing temperature is increased due to the diffusion of boron atoms.

5.4 Kinetic of Atom Diffusion Analysis

It is important to calculate the thickness of boride layer because it has to be substituted in Eq (3.2) in order to get the squared boride layer thickness. From the graph of squared boride layer thickness as in Figure 4.5 (subsection 4.3), the gradient for each temperature can be obtained. After fitting the logarithmic values of the average thickness for the boride layer as a function of inverse temperatures, the diffusion activation energy can be defined from the slope of the straight line presented in Figure 4.6.

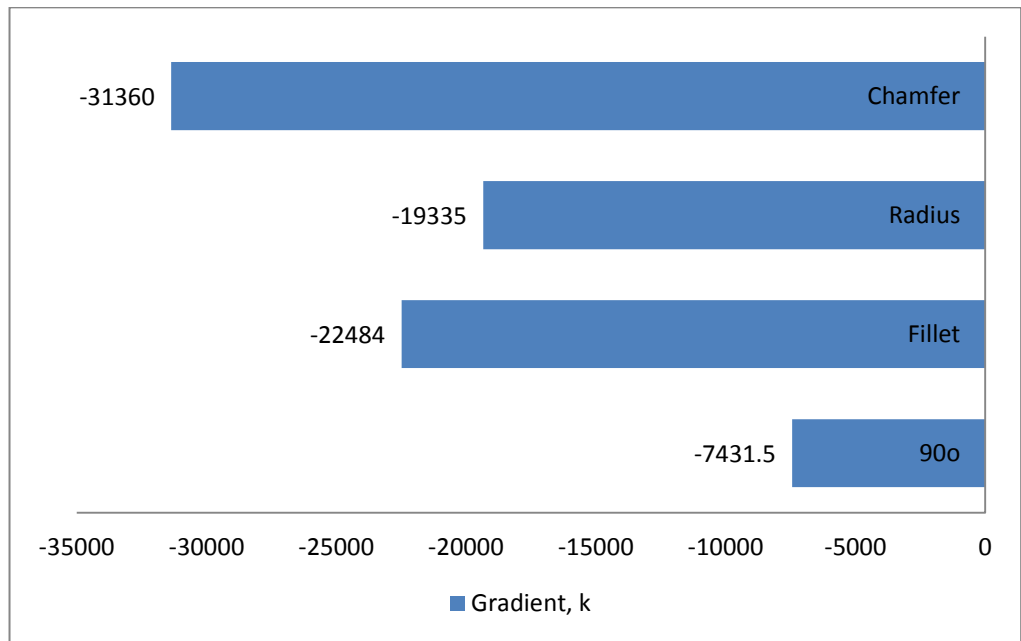


Figure 5.3 Chart for gradient of geometries

The plot of $\ln k$ as a function of the reciprocal temperature exhibits a linear relationship according to the Arrhenius Equation. The gradient value for the 90°, fillet, radius and chamfer is -7431.5, -22484, -19335 and -31360 respectively as in Figure 5.3 below. Then the activation energy can be obtained by rearranged Eq (2.2).

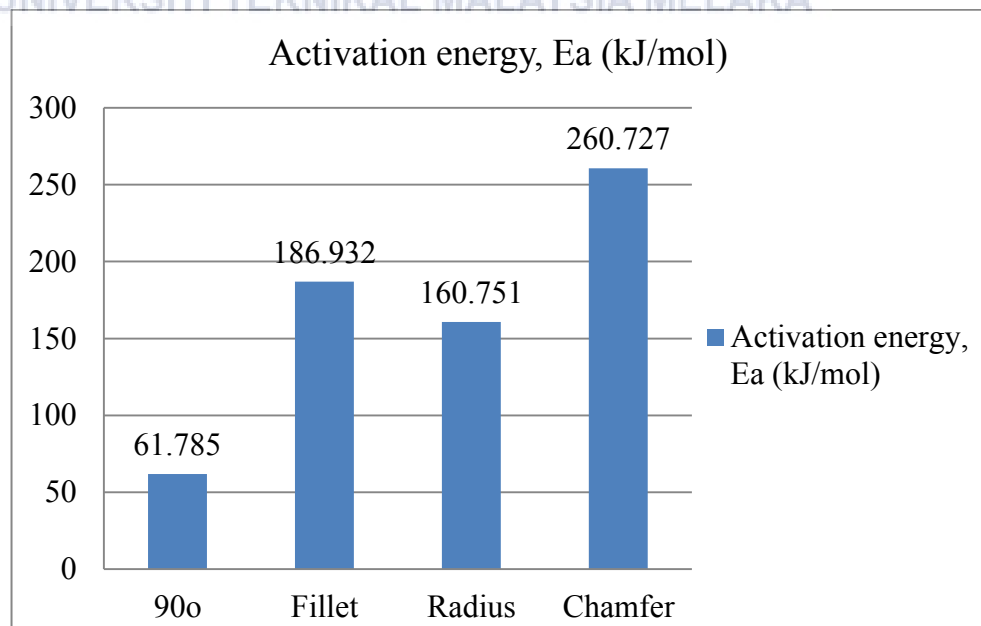


Figure 5.4 Graph of activation energy for four geometries

Figure 5.4 below shows the activation energy of 61.785 kJ/mol, 160.751 kJ/mol, 186.932 kJ/mol, and 260.727 kJ/mol for 90°, radius, fillet, and chamfer geometry respectively. From the obtained value of the activation energy it shows that the 90° geometry has the lowest activation energy and it is the best geometry for the effective boronizing process. This is because of the 90° geometry may have the packed boron during the boronizing process. The sharp edges make the diffusion easier to happen at that geometry.

The second lowest activation energy is the radius geometry with the value of 160.751 kJ/mol. This is because of the radius of the geometry is 5mm and the large corner surface make the diffusion easy to happen compared with the fillet that has activation energy of 186.932 kJ/mol that are higher than the radius geometry. This is caused by the fillet surface which is small, with dimension of 1mm and need more energy for diffusion to happened. The chamfer geometry shows the highest value for the activation energy that is 260.727 kJ/mol. This might cause from the shape that makes the boron hard to diffuse compared with three others geometry.

From the Figure 5.4, it shows all the four geometry and their activation energy value. It shows that the 90° geometry have the lowest activation energy and make the boron easy to diffuse. This study have been achieved the objective where to find which part of the geometries shows the most effective boronizing process by rate of activation energy. This result can be suggested to the industries so that they can apply it in their products.

CHAPTER 6

CONCLUSION AND RECOMMENDATIONS

6.1 Introduction

In this chapter, the result and discussion will be concluded and based on the result, it will show either the objectives of this study have been achieved or not. Based on this study, there will be improvement that can be made and other suggestions for further study will be discussed in the recommendations.

6.2 Conclusion

Boronizing is known to be widely used in industrial applications. For this study, the material for the boronizing process is mild steel and the compositions of the material have been studied. In this study, the sharp cornered surface will be studied in order to know which part of the geometries that shows the most effective boronizing process by analyzing the rate of diffusion.

From the literature review, there are much information about the boronizing process and the microstructure for the material. The specimens for boronizing have been successfully designed and fabricated. After the boronizing process, the material characterization processes have been followed to get the microstructure and thickness of boride layer. Based on the result that have been calculated and plotted as in Chapter 4, Data and result and Chapter 5, Discussion and analysis it can be conclude that,

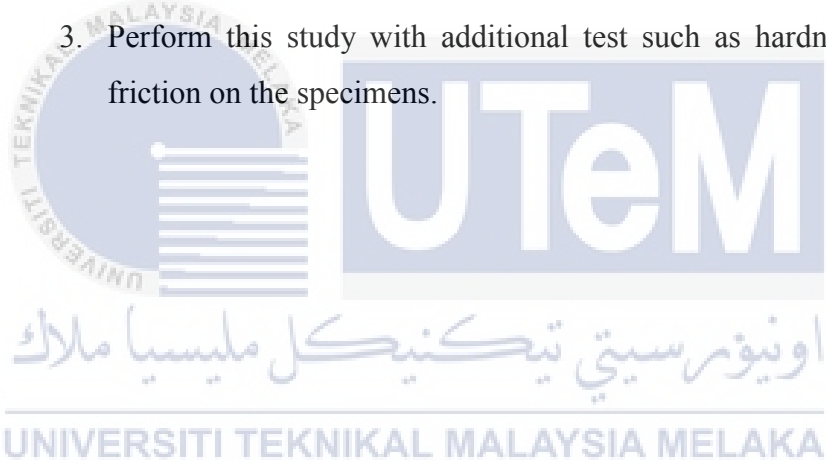
1. The lowest activation energy is at the 90° geometry compared with three others geometry with the reading 61.785 kJ/mol as in Figure 5.4.
2. This shows that the 90° geometry is the most effective for boronizing process because it has the lowest activation energy.
3. This result can be suggested to the industries to improve their product and design.

This study managed to achieve the objectives as in Chapter 1, Introduction, that are to study the effect of boronizing in temperature and time on the sharp cornered surface using the metallographic analysis and to analyse the effect of different cornered geometries on the boronizing diffusion using the activation energy analysis.

6.3 Recommendations

There are some recommendations that can be recommend for further study based on this study and it can be used to improve this study. It can be suggested that,

1. By using this study, try different geometries to see if there are other geometries have better activation energy compared with this study.
2. Apply the boronizing process to other types of steel such as stainless steel in order to compare the behavior and activation of energy for the best shape.
3. Perform this study with additional test such as hardness, wear and friction on the specimens.



REFERENCES

Arthur & Alexander, W.O. (1944). *Metals in the Service of Man*. 11th Edition (1998-2016). *General Properties of Steel*. The American Iron & Steel Institute, www.steel.org

ASTM (1998-2016). Retrieved from <https://www.astm.org/Standards/steel-standards.html>

Béjar, M. A., & Moreno, E. (2006). Abrasive wear resistance of boronized carbon and low-alloy steels. *Journal of Materials Processing Technology*, 173(3), 352–358.

Bell, T. (2016, August 16). What are the different types of steel? Retrieved from <https://www.thebalance.com/steel-grades-2340174>

Campos, I., Ramírez, G., Figueroa, U., & Velázquez, C. V. (2007). Paste boriding process: evaluation of boron mobility on borided steels. *Surface Engineering*, 23(3), 216-222.

Kelemenis, G. (2003). Kinetic study of boron diffusion in the paste-boriding process. *Materials Science and Engineering: A*, 352(1-2), 261-265.

Chegroune, R., Keddou, M., Abdellah, Z. N., Ulker, S., Taktak, S., & Gunes, I. (2016). Characterization and kinetics of plasma-paste-borided AISI 316 steel. *Materiali in tehnologije*, 50(2), 263-268.

Çulha, O. (2006). *Dokuz Eylül University Graduate School Of Natural And Applied Sciences Determination Of Thin Film's Mechanical Properties*. Retrieved from http://www.fbe.deu.edu.tr/all_files/tez_arsivi/2007/yl_t2130.pdf

Davis, J.R.(R.). 2002, Surface hardening of steels: understanding the basics, ASM International, Materials Park, OH.

Dunlap, M., & Adaskaveg, D. J. E. (1997). *Introduction to the scanning electron microscope*. Retrieved from <https://imf.ucmerced.edu/downloads/semmanual.pdf>

Educastur. (2009). Non-ferrous metals. Retrieved from <http://blog.educastur.es/tecnoinfiesto/files/2009/05/theory-metals.pdf>

Genel, K., Ozbek, I., & Bindal, C. (2003). Kinetics of boriding of AISI W1 steel. *Materials Science and Engineering: A*,347(1-2), 311-314.

He, X., Xiao, H., Ozaydin, M. F., Balzuweit, K., & Liang, H. (2015). Low-temperature boriding of high-carbon steel. *Surface and Coatings Technology*,263, 21-26..

Gunes, I., & Ozcatal, M. (2015). Diffusion kinetics and characterization of borided AISI H10 steel. *Materiali in tehnologije*,49(5), 759-763.

Inc, O. A. (2012). Anatomy of the microscope-introduction.. Retrieved from <http://www.olympusmicro.com/primer/anatomy/introduction.html>

Ipek, M., Celebi Efe, G., Ozbek, I., Zeytin, S., & Bindal, C. (2012). Investigation of Boronizing Kinetics of AISI 51100 steel. *Journal of Materials Engineering and Performance*, 21(5), 733–738.

Jain, V., & Sundararajan, G. (2002). Influence of the pack thickness of the boronizing mixture on the boriding of steel. *Surface and Coatings Technology*,149(1), 21-26.

Jeol. (2009). *SEM SEM scanning electron microscope A to Z serving advanced technology*. Retrieved from http://www.jeol.co.jp/en/applications/pdf/sm/sem_atoz_all.pdf

K y l Y ün ş U l S (2012) D ff on k n of bo d d A S 52100 nd A S 440C steels. *Vacuum*,86(10), 1428-1434.

Küper, A., Qiao, X., Stock, H. R., & Mayr, P. (2000). A novel approach to gas boronizing. *Surface and Coatings Technology*, 130(1), 87–94.

Li, C., Shen, B., Li, G., & Yang, C. (2008). Effect of boronizing temperature and time on microstructure and abrasion wear resistance of Cr12Mn2V2 high chromium cast iron. *Surface and Coatings Technology*, 202(24), 5882-5886.

Metals, C. (2012, July 31). Ferrous & Non-Ferrous metals and their uses. Retrieved from <http://www.castlemetalseurope.com/blog/ferrous-nonferrous-metals-uses/>

Mukhopadhyay, S. M. (2003). Sample preparation for microscopic and spectroscopic characterization of solid surfaces and films. *Sample Preparation Techniques in Analytical Chemistry*.

Omar, N. H., Hasan, R., & Masripan, N. A. B. (2016). *Kinetic study of boron diffusion in powder-pack boronizing*

Thallesthadeu, /. (2014, December 14). Boriding. Retrieved from <https://matenggroup.wordpress.com/2014/12/05/boriding/>

The Editors of Encyclopædia Britannica (2015). Activation energy | chemistry. In *Encyclopædia Britannica*. Retrieved from <https://global.britannica.com/science/activation-energy>

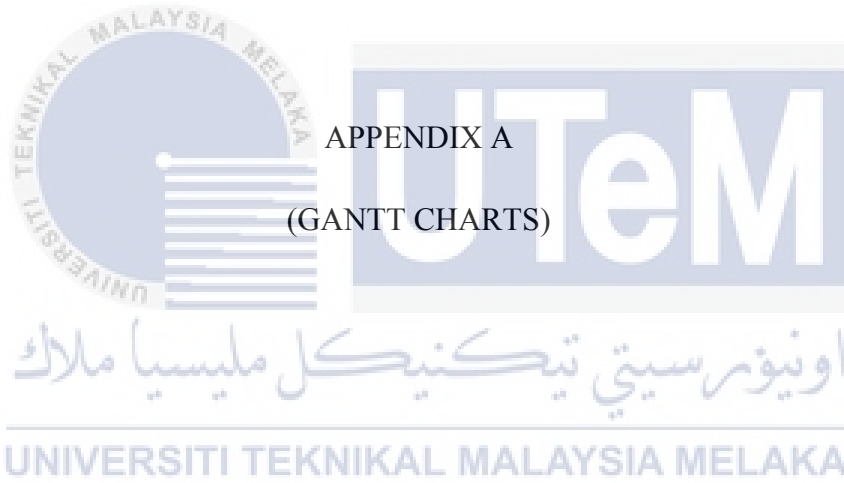
Wear protection with Borocoat-Diffusion layers (2016). Retrieved from <http://avionmfg.com/pdfs/Boronizing-AVION.pdf>

Xu, J. (2014). *MSE 5034 spring 2004*. Retrieved from <http://www.eng.utah.edu/~lzang/images/lecture-3.pdf>

Y n H P W X M n Y A W T R Z 2013 “Pl m bo d n of high strength alloy steel with nanostructured surface layer at low temperature assisted by air bl ho p n n” S f o n T hnolo y vol 228 pp 229

Yu, L. G., Khor, K. A., & Sundararajan, G. (2002). Boriding of mild steel using the spark plasma sintering (SPS) technique. *Surface and Coatings Technology*, 157(2-3), 226–230.





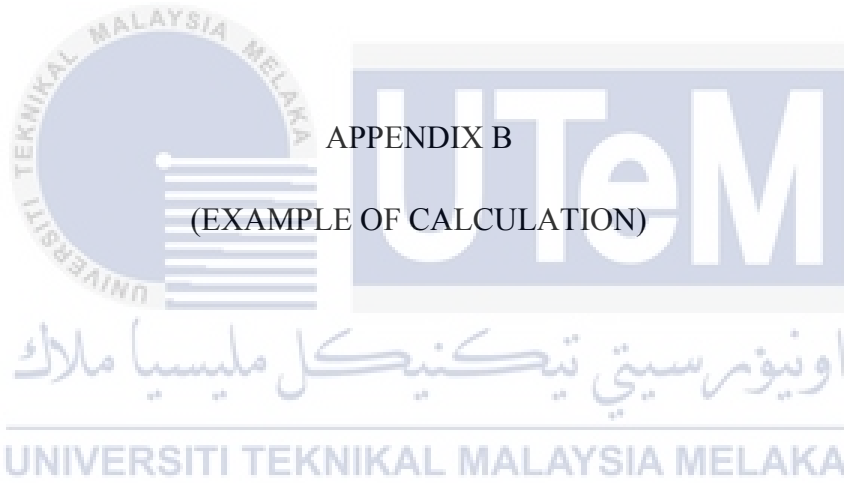
Gantt Charts for PSM 1

NO	TASK	WEEK																
		1	2	3	4	5	6	7	8	9	10	11	12	13	14	15	19	
1	Title Confirmation	█																
2	Check for material		█															
3	Chapter 1: Introduction			█	█	█	█											
4	Design the specimen					█	█	█										
5	Submission progress report 1								█									
6	Fabricate the specimen									█	█	█	█					
7	Literature review										█	█	█	█				
8	Methodology													█	█			
9	Conclusion														█			
11	PSM 1 submission report																█	
12	Presentation/seminar																	█

Gantt Charts for PSM 2

NO	TASK	WEEK															
		1	2	3	4	5	6	7	8	9	10	11	12	13	14	15	16
1	Boronizing process	█	█	█													
2	CNC milling				█	█	█										
3	Grinding and polishing						█	█			█	█					
4	Progress report submission							█									
5	Scanning Electron Microscope									█	█	█					
6	Result and data										█	█	█				
7	Conclusion											█	█	█			
8	PSM 2 submission report														█		
9	Slide preparation															█	
11	Presentation/seminar																█





APPENDIX B

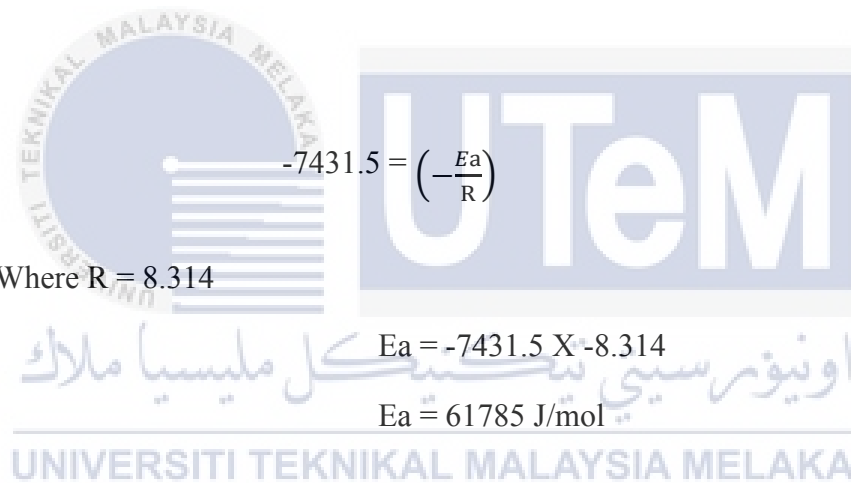
(EXAMPLE OF CALCULATION)

To calculate the activation energy based on the gradient from the graph

Geometry	Gradient, k
90°	-7431.5
Fillet	-22484
Radius	-19335
Chamfer	-31360

$$k = Ae^{\left(\frac{Ea}{RT}\right)}$$

Example:



$-7431.5 = \left(\frac{Ea}{R}\right)$

Where $R = 8.314$

$Ea = -7431.5 \times -8.314$

$Ea = 61785 \text{ J/mol}$

UNIVERSITI TEKNIKAL MALAYSIA MELAKA



APPENDIX C
(TABLES)



اونيورسيتي تيكنيكل مليسيا ملاك

UNIVERSITI TEKNIKAL MALAYSIA MELAKA

90D

Temperature (K)	Time (Hour)											
	2				4				6			
	1	2	Average	Standard deviation	1	2	Average	Standard deviation	1	2	Average	Standard deviation
1123	61.8	54.8	58.3	4.9	40.3	88.0	64.1	33.7	49.4	80.7	65.0	22.2
1173	72.4	46.0	59.2	18.7	86.8	45.6	66.2	29.1	109.3	30.2	69.8	56.0
1223	69.7	52.1	60.9	12.5	84.5	49.3	66.9	24.9	90.2	53.0	71.6	26.3

1MM FILLET

Temperature (K)	Time (Hour)											
	2				4				6			
	1	2	Average	Standard deviation	1	2	Average	Standard deviation	1	2	Average	Standard deviation
1123	50.3	26.8	38.6	16.6	54.7	36.7	45.7	12.7	62.8	30.3	46.6	23.0
1173	32.2	51.2	41.7	13.5	81.1	30.3	55.7	35.9	81.5	34.2	57.9	33.4
1223	76.9	35.2	56.0	29.5	111.7	40.4	76.0	50.4	117.8	45.1	81.5	51.4

5MM RADIUS

Temperature (K)	Time (Hour)											
	2				4				6			
	1	2	Average	Standard deviation	1	2	Average	Standard deviation	1	2	Average	Standard deviation
1123	60.1	44.6	52.4	11.0	28.0	78.2	53.1	35.5	71.2	45.1	58.2	18.5
1173	36.6	73.2	54.9	25.9	52.5	75.2	63.9	16.0	47.0	81.5	64.3	24.4
1223	75.7	48.1	61.9	19.5	128.5	30.0	79.2	69.6	43.7	117.3	80.5	52.1

CHAMFER

Temperature (K)	Time (Hour)											
	2				4				6			
	1	2	Average	Standard deviation	1	2	Average	Standard deviation	1	2	Average	Standard deviation
1123	82.5	48.7	65.6	23.9	45.0	88.2	66.6	30.5	38.1	97.3	67.7	41.8
1173	45.4	83.9	65.6	27.2	70.7	63.5	67.1	5.0	60.5	98.8	79.7	27.1
1223	54.5	87.0	70.8	23.0	57.3	89.6	73.5	22.8	74.6	101.2	87.9	18.8